Abdominal Radiology

Published online: 9 August 2016

Abdom Radiol (2017) 42:987–1019
DOI: 10.1007/s00261-016-0859-8

Abdominal radiograph pearls and pitfalls for the emergency department radiologist: a pictorial review

Jerry T. Loo,[1,2,3] Vinay Duddalwar,[1] Frank K. Chen,[1] Tapas Tejura,[1] Ilya Lekht,[1] Mittul Gulati[1]

[1]Department of Radiology, USC Keck School of Medicine, 1500 San Pablo Street, 2nd Floor Imaging, Los Angeles CA 90033, USA
[2]Department of Radiology, LAC-USC Medical Center, 1200 N. State Street, D&T 3D321, Los Angeles, CA 90033, USA
[3]Department of Radiology, David Geffen School of Medicine, University of California, Los Angeles (UCLA), 757 Westwood Plaza, Ste 1638, Los Angeles, CA 90095, USA

Abstract

Abdominal plain films are often the first imaging examination performed on a patient with abdominal pain in the emergency department. Radiograph findings can help guide clinical management and the need for advanced imaging. A pictorial review of a range of abdominal radiograph findings is presented, including bowel gas patterns, abdominal organ evaluation, pathologic gas, calcifications, implanted devices, and foreign bodies.

Key words: Abdominal plain film—Emergency radiology—Acute abdomen—Gas patterns—Calcifications—Foreign bodies

Acute abdominal pain is the reason for 8% of emergency department (ED) visits [1]. In the ED, abdominal radiographs are frequently the initial imaging examination obtained for evaluation of acute abdominal pain [2]. Data on the number of ED patients with abdominal pain who undergo radiographs are not available. However, to illustrate their prevalence, abdominal radiographs are performed on 75% percent of patients clinically suspected of having acute appendicitis. This is despite evidence that radiographs have no diagnostic value in these patients [3].

Multiple studies have found the role of abdominal plain films to be limited in the adult ED because the physician's clinical diagnosis and level of confidence rarely changed after the abdominal radiographs [4, 5]. Bowel obstruction, renal colic, and generalized abdominal pain are the most common indications for performing an abdominal plain film in the ED [4]. Of these entities, abdominal radiographs increase the sensitivity for detecting small bowel obstruction only [5]. In addition, advanced imaging (CT, US, MRI) revealed abnormalities that were not apparent on radiographs in 80% of patients [4]. Some authors went on to suggest that the greatest utility in ED abdominal plain films may be the evaluation of line and tube positioning given the lack of sensitivity and specificity in detecting many acute abdominal pathologies compared with CT [4]. Despite these conclusions, the true value of abdominal plain films in the ED may actually be more nuanced. For example, in the study by Kellow [4], ED physicians did not seek advanced imaging following a normal abdominal plain film about 20% of the time—a large number of patients in any high volume ED. In these patients, the information provided by the negative plain film was sufficient to continue treatment without further imaging workup [6]. The conclusions suggest that in a subset of ED patients, including those with a relatively benign history and physical examination, the plain film may reassure the ED physician and accelerate empiric treatment and patient discharge. The value of abdominal plain films in the pediatric population has also been studied. For example, the utility of plain film in pediatric ED patients is demonstrated by the frequent need to detect ingested metallic foreign bodies [7]. Furthermore, ionizing radiation from CT should be limited in pediatric patients, and the lower doses from radiographs have been documented [8].

Most abdominal radiographs are taken in the anterior–posterior (AP) projection, with the film placed behind the supine patient, and the X-ray beam passing from the front

Correspondence to: Jerry T. Loo; *email:* jerryloo@usc.edu

Table 1. Abdominal radiograph recommended search pattern

1. Demographics (name, age, sex)
2. Technical assessment (projections, body position, markers, limitations)
3. Systematic review (ordered by personal preference):
   a. Medical devices or implants
   b. Organs (liver, spleen, kidneys, psoas muscles, bladder)
   c. Gastrointestinal tract (stomach, small bowel, colon)
   d. Soft tissues
   e. Bones
   f. Abnormal calcifications or densities (vascular, lymph nodes, calculi)

to the back. In comparison with supine radiographs, upright or left lateral decubitus studies are more sensitive for detection of free intraperitoneal air [9]. The delivered radiation dose from abdominal radiographs is limited (0.1–1.0 mSv) compared to that of computed tomography (CT) of the abdomen and pelvis (10–15 mSv) [10].

As with other imaging studies, a step-by-step approach to image analysis improves diagnostic accuracy [9]. A recommended search pattern for abdominal radiographs is provided (Table 1). An illustrated overview of bowel gas patterns, abdominal organ evaluation, pathologic gas, calcifications, implanted devices, and foreign bodies follows, to serve as a guide to abdominal radiograph interpretation.

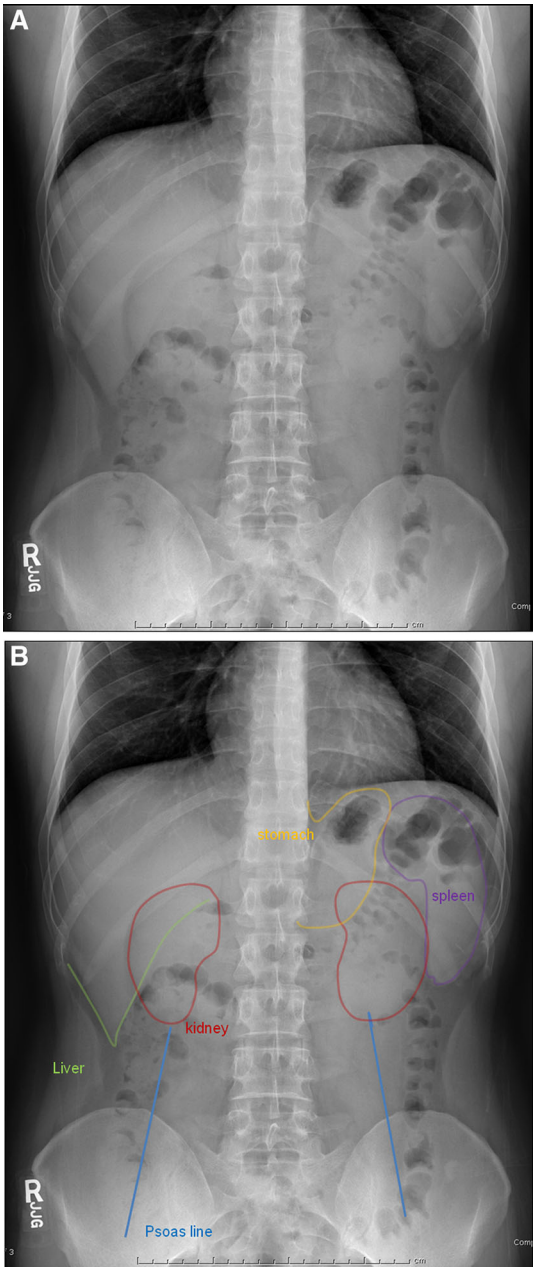

Fig. 1. **A** Normal abdominal radiograph. **B** Liver (*green*), spleen (*purple*), kidneys (*red*), stomach (*orange*), and psoas muscles (*blue*).

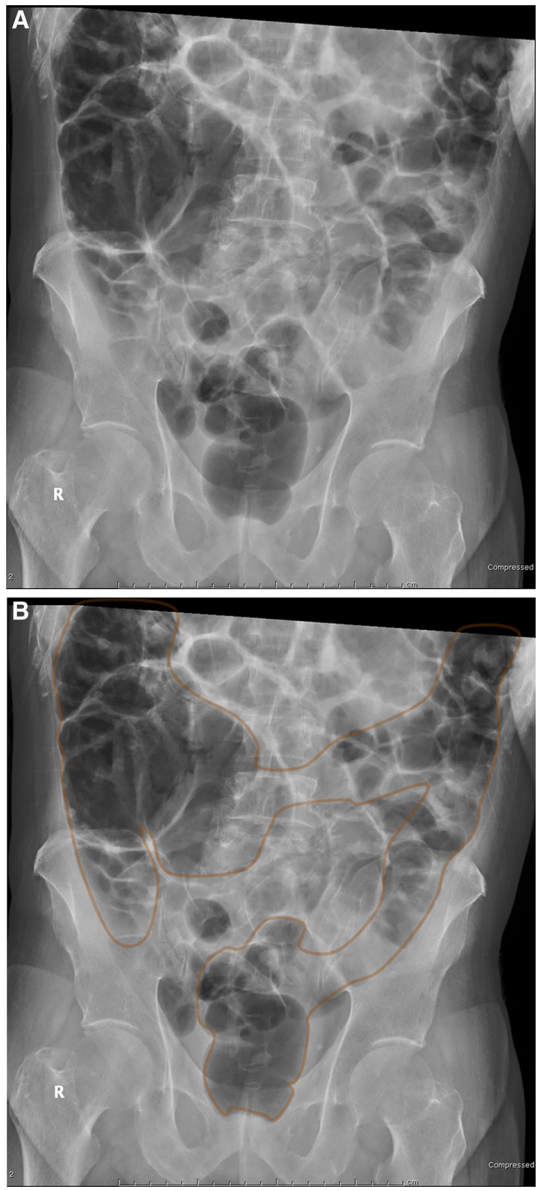

Fig. 2. **A** Abdominal radiograph demonstrating distention of small and large bowel consistent with generalized ileus. **B** Large bowel gas outlined (*brown*).

Bowel gas patterns

On a normal abdominal X-ray, the borders of the liver, spleen, kidneys, stomach, and psoas muscles are all clearly delineated (Fig. 1). The liver presents as a large triangular soft tissue density in the right upper quadrant abutting the undersurface of the diaphragm, usually displacing the bowel away unless there is colonic interposition (Chilaiditi sign) [11]. Overlying lower lobe lung markings are frequently visible and should not be confused with pathology in the liver. The spleen is represented by a bean-shaped soft tissue density in the left upper quadrant and is not always reliably seen on plain film. Kidneys are also bean-shaped soft tissue densities with smooth contours, usually extending from about the level of T12 to L2-L3. Of note, the left kidney is slightly higher in position compared to the right due to mass effect from the liver. The stomach is demarcated by an air–fluid level underneath the left hemidiaphragm on erect radiographs. On supine films, pooling liquid in the

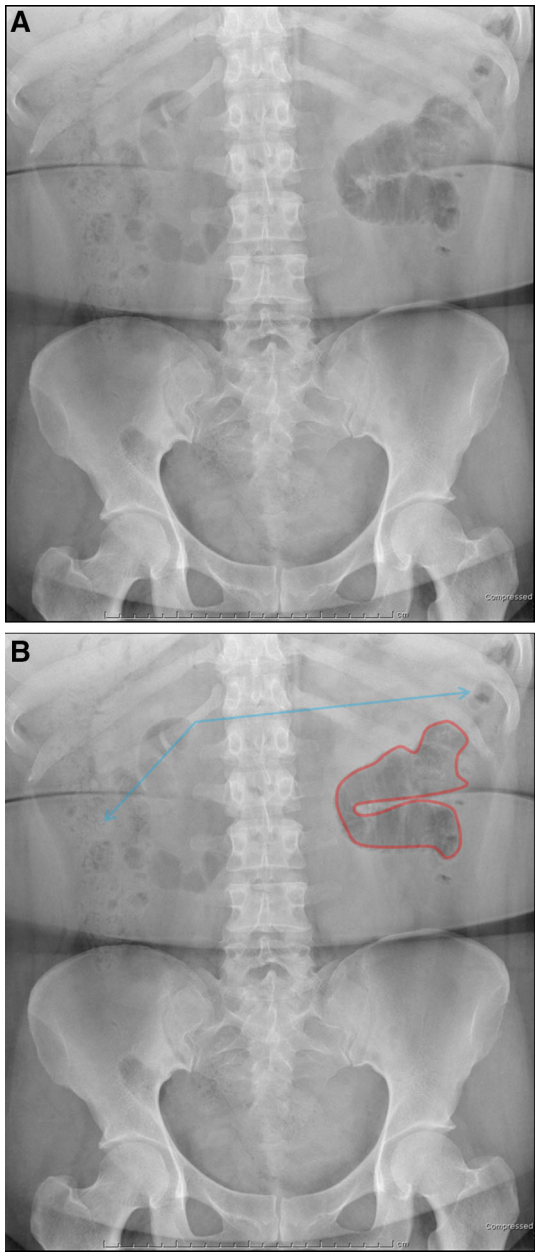

Fig. 3. **A** Abdominal radiograph demonstrating localized ileus. **B** Sentinel loop (*red*), normal gas in the colon (*blue*).

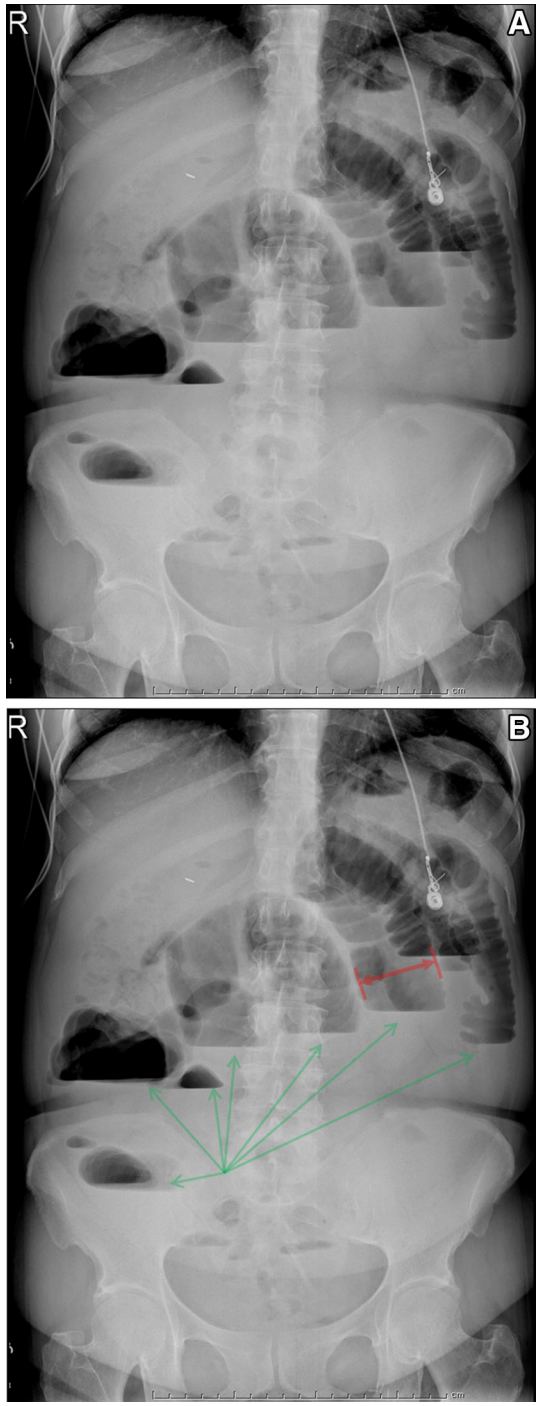

Fig. 4. **A** Abdominal radiograph demonstrating small bowel obstruction. **B** Dilated small bowel segment (*red*), air–fluid levels (*green*).

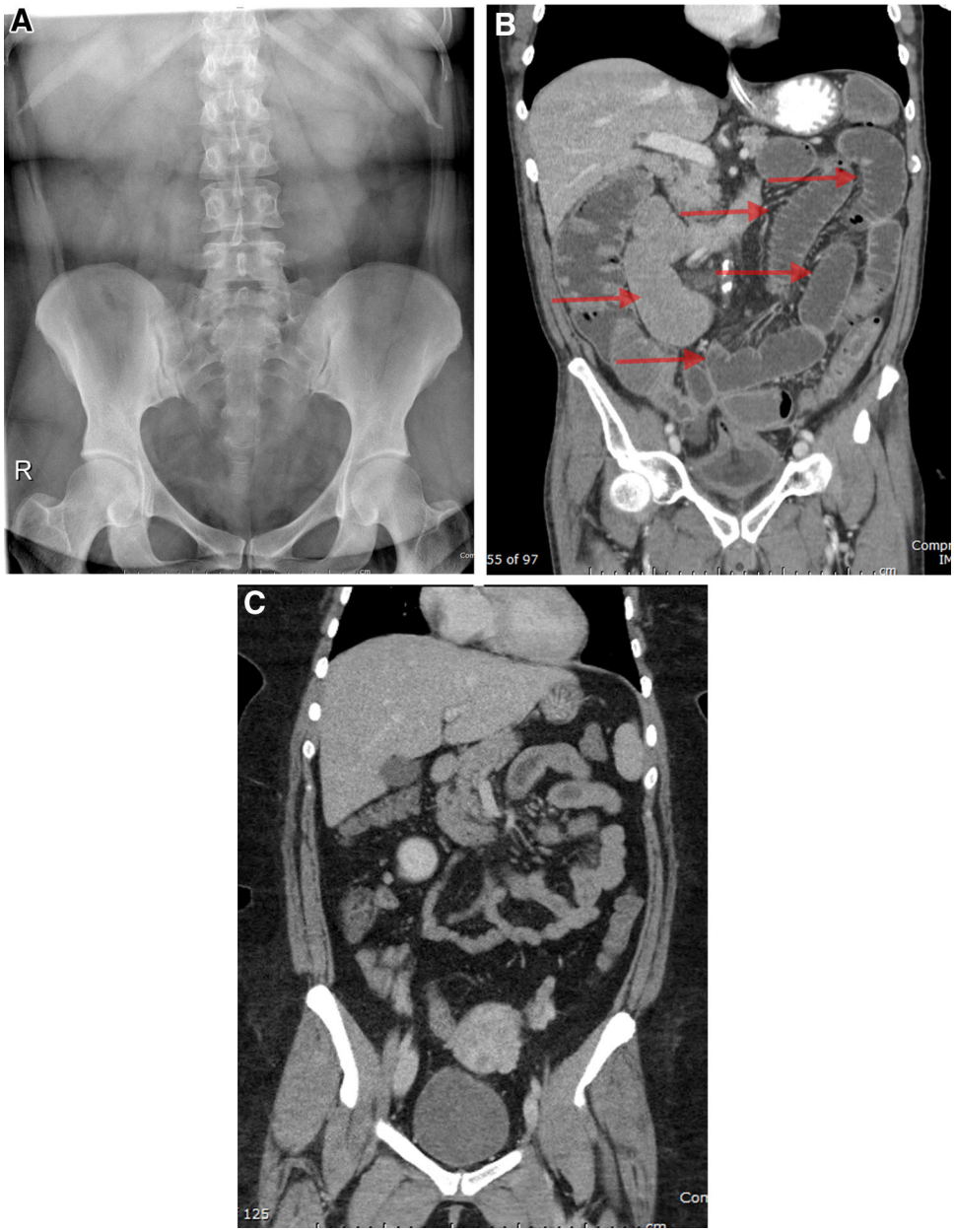

Fig. 5. **A** Abdominal radiograph demonstrating a "gasless" abdomen. **B** Coronal CT abdomen and pelvis showing numerous fluid-filled segments of small bowel (*red arrows*). **C** Coronal CT showing normal decompressed bowel. Patients in Fig. 5B, C were different people, and both had gasless abdomens on plain film.

gastric fundus may present as a circular soft tissue outline that disappears or changes depending on patient position. The psoas muscles form two straight diverging lines extending inferolaterally from the lumbar spine to their insertion on the lesser trochanters of the femurs. They can be obscured by overlying gas or a paucity of surrounding fat. Within the pelvis, the bladder can sometimes be seen as a midline ovoid soft tissue density mass, provided it is distended with enough urine. Gas and fecal material are frequently seen within normal caliber large bowel.

Pathologic patterns of bowel gas include ileus, which can be generalized or localized; small and large bowel obstruction; and volvulus types, of which sigmoid volvulus is the most common. A generalized ileus refers to a disruption in the normal coordinated propulsive motor activity of the entire gastrointestinal tract from some nonmechanical insult such as surgery, inflammation, or other neural or metabolic cause [12]. On plain film, a generalized ileus will present as multiple air distended loops of small and large bowel, most commonly seen in postoperative patients. The borders of the dilated

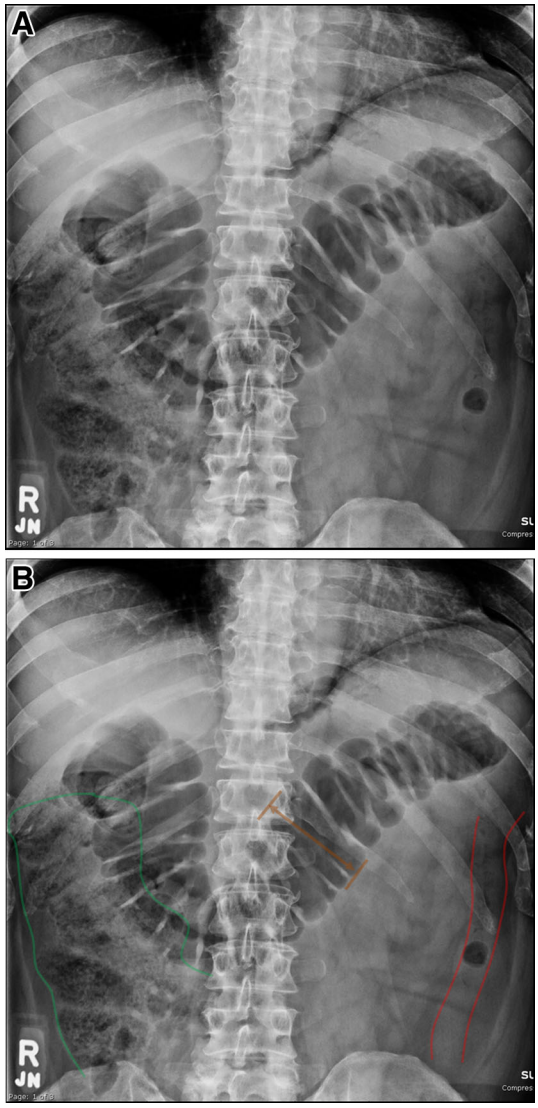

Fig. 6. **A** Abdominal radiograph demonstrating large bowel obstruction. **B** Dilated proximal large bowel (*green*), dilated transverse colon (*brown*), collapsed distal colon (*red*).

large bowel are highlighted to differentiate from small bowel distention (Fig. 2). Dilated small bowel loops measuring greater than 3 cm and colon measuring greater than 6 cm are common findings in ileus; the more distensible cecum can normally measure up to 10 cm [13]. Some authors have reported 96% sensitivity and 82% specificity for detecting small bowel ileus versus obstruction on abdominal plain film [14]. Typically, no more than two small air–fluid levels with comparable heights should be seen in ileus, otherwise an obstruction should be suspected. Pascal's Principle states that the pressure within a cylindrical structure is the same, regardless of whether the structure is dilated [15]. Thus, in an ileus, equal height air–fluid levels in the bowel have "found their level" and may appear to be *U*-shaped, implying no obstruction and both ends being exposed to equal pressure in the bowel lumen.

A localized ileus (Fig. 3) can be the result of an adjacent inflammatory or infectious process. On plain film, a localized ileus can present as a focal cluster of one to three distended and/or mildly dilated loops of small bowel. These loops have been termed "sentinel loops," and their location in the abdomen can help narrow the differential or suggest an underlying etiology. For example, left abdominal sentinel loops of dilated jejunum have been associated with acute pancreatitis [16]. Gas in the distal colon/rectum makes the presence of a complete small bowel obstruction unlikely [17].

Small bowel obstruction (SBO) has a variety of etiologies, the leading cause being postoperative adhesions. As fibrous bands block transit through extrinsic compression, secretions and air accumulate, stimulating further secretions. Resulting clinical symptoms include vomiting, distention, and abdominal pain [18]. Some studies show CT is superior to plain film in diagnosing SBO, while others show the two are comparable [19, 20]. For example, in the study by Maglinte et al. [21], the sensitivity and specificity of plain film radiography for revealing SBO were 69% and 57%, respectively, similar to a CT scan, when equal numbers of low- and high-grade obstructions were included [18, 21]. The benefit of CT over plain film lies in its ability to accurately reveal the underlying etiology of a SBO 95% of the time [21]. On plain film, a complete SBO can be seen as multiple dilated (>3 cm) loops of small bowel with multiple air–fluid levels on an upright radiograph (Fig. 4). In contrast to an adynamic ileus, multiple uneven or "*J*-shaped" air–fluid levels may be seen, suggesting obstruction and unequal pressurization at opposite ends of the fluid levels. The sensitivity and specificity of these uneven fluid levels for the diagnosis of SBO are 53% and 71%, respectively [22]. Signs of a high-grade SBO include more than two air–fluid levels—air–fluid levels wider than 2.5 cm, and those differing more than 2 cm in height. In addition, there should be a paucity of gas distally in the large bowel [17].

Sometimes an adult abdominal plain film may show little or no bowel gas, termed a "gasless abdomen." This is a "nonspecific" finding seen in a range of etiologies from benign to threatening. Clinical history plays a key role in distinguishing these entities from each other. Beginning with benign causes, many healthy patients ingest very little air and naturally have sparse bowel gas. Patients who have had a total colectomy also commonly have little small bowel gas for unknown reasons. Infec-

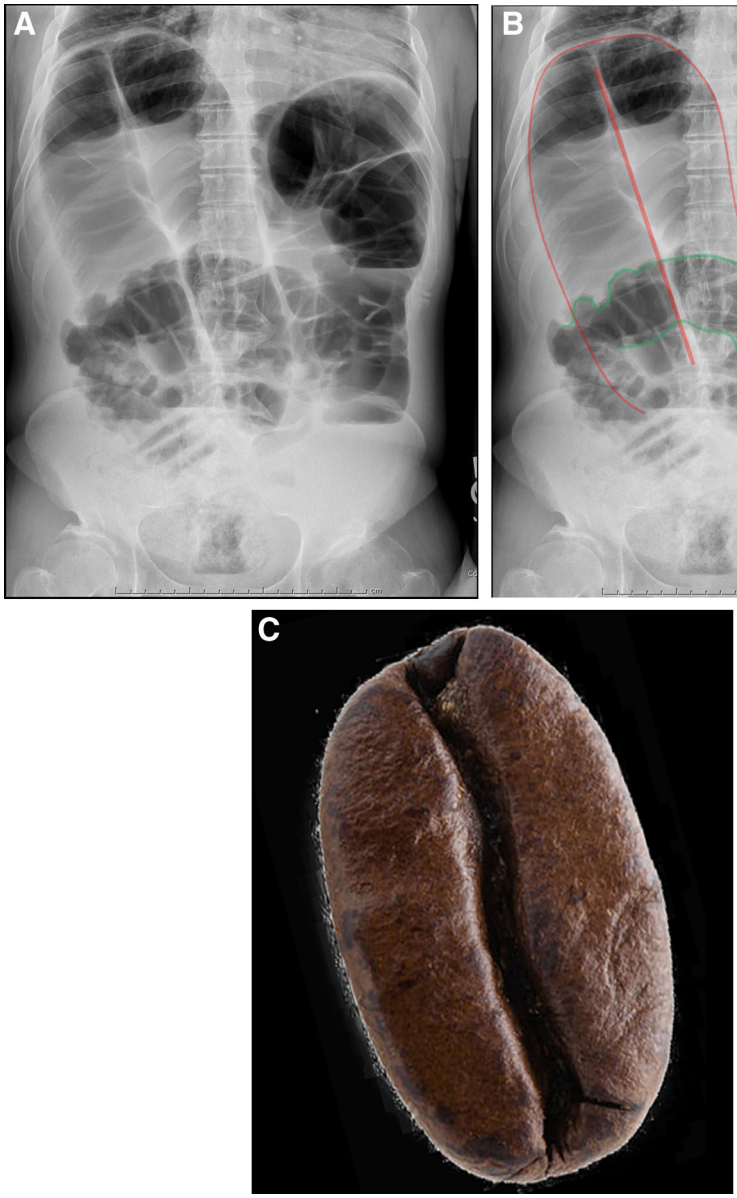

Fig. 7. **A** Abdominal radiograph demonstrating sigmoid volvulus. **B** Northern exposure sign (*red*), transverse colon (*green*). **C** Coffee bean (*picture*).

tious or inflammatory enteritis can lead to excessive secretions and diarrheal disease that distends the bowel with fluid and obliterates the normal bowel gas pattern. A very proximal small bowel obstruction leading to distal decompression or development of multiple dilated fluid-filled segments will often produce a gasless abdomen on a supine film (Fig. 5). Subsequent upright films demonstrating multiple air–fluid levels may confirm the diagnosis. Finally, a large intra-abdominal mass or volume of ascites may displace and obscure bowel gas [23].

Large bowel obstruction (LBO) is frequently seen in the setting of colon cancer [24]. On plain film, there is dilatation of the proximal large bowel, with accumulation of gas and feces (Fig. 6). The distal colon beyond the site of obstruction may be collapsed, helpful to differentiate LBO from ileus. The colon proximal to the obstruction is often dilated to greater than 6 cm, and the cecum to greater than 10 cm. Given that the cecum has the largest diameter in the normal colon, this is in keeping with Laplace's law, paraphrased to state that pressure needed to distend a hollow viscus varies inversely with its radius [25].

Sigmoid volvulus is more common in older patients. Risk factors include age, a history of chronic constipation, and high fiber diets—all of which can lead to redundancy of the sigmoid colon [26]. Plain film sensi-

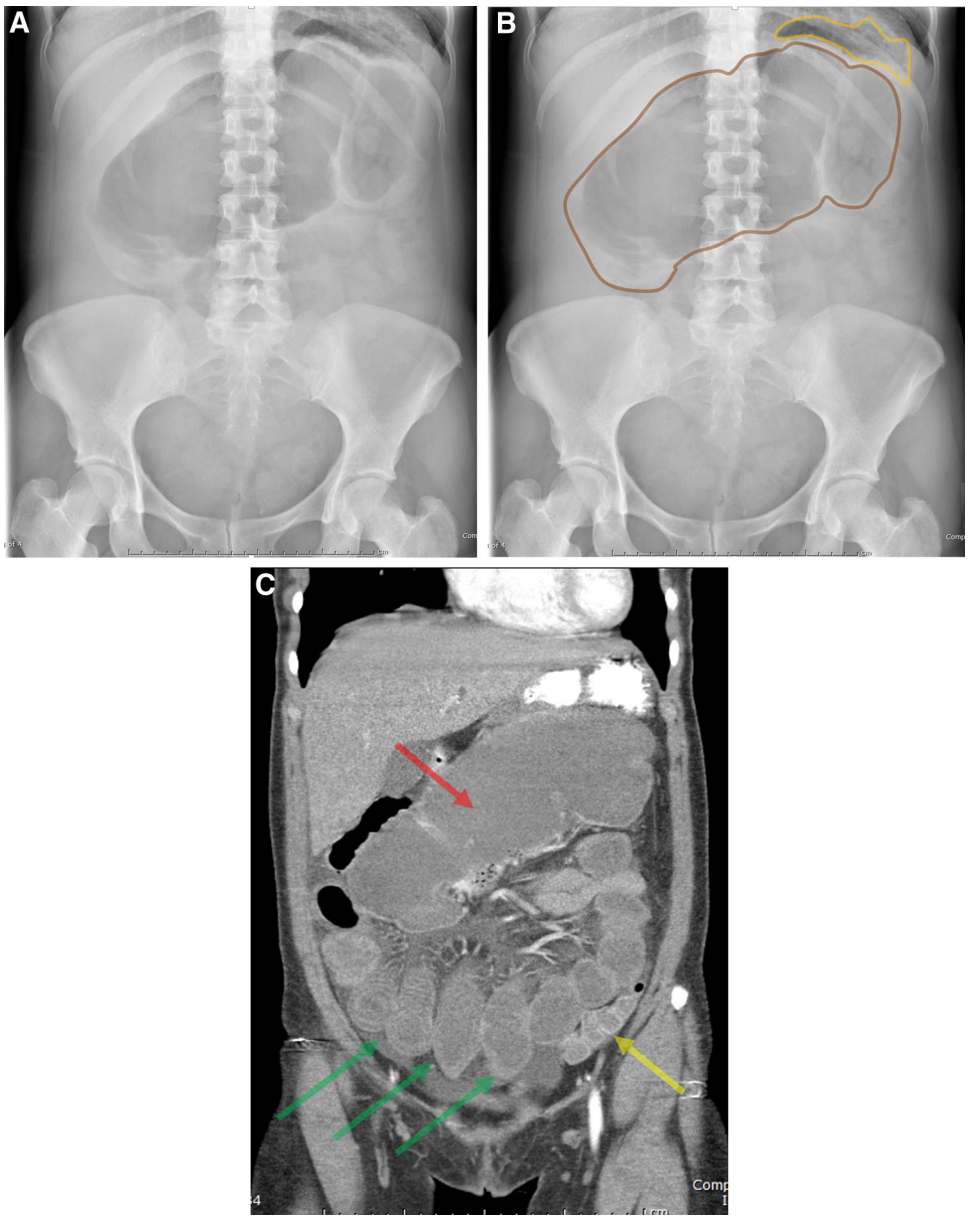

Fig. 8. **A** Abdominal radiograph demonstrating cecal volvulus. **B** Dilated, centrally displaced cecum with persistent colonic haustral markings (*brown*), stomach bubble in the *left upper* quadrant (*yellow*). Note the paucity of small bowel and distal colonic gas, concerning with obstruction. **C** Coronal CT demonstrating a fluid-filled dilated cecum (*red arrow*), thickened, edematous upstream small bowel (*green arrow*), decompressed distal sigmoid colon (*yellow arrow*).

tivity for sigmoid volvulus can range anywhere from 57% to 90% [27]. Sigmoid volvulus is a surgical emergency and can lead to strangulation and bowel necrosis [28]. On plain film (Fig. 7), classic findings include a coffee bean (inverted "*U*") appearance (sensitivity 88%, specificity 80%), with a vertical dense line formed from the inner walls of the two segments of apposed colon where the normal haustral markings are lost [29], [30]. A "northern exposure" sign (sensitivity 86%, specificity 100%) may also be seen, in which the apex of the dilated sigmoid rises above the transverse colon and points toward the right hemidiaphragm [31].

Cecal volvulus is an unusual entity, representing only 1%–3% of all intestinal obstructions but 10%–30% of colonic volvulus [32]. Plain film sensitivity for cecal volvulus can reach 75% [27]. Three types of cecal volvulus have been described on CT: axial torsion (Type 1), loop (Type 2), and the cecal bascule (Type 3) [32]. Distinguishing these entities on plain film is not feasible as it requires careful analysis of twisting and bowel folding patterns, best seen on cross-sectional imaging. The key to diagnosing cecal volvulus on plain film is recognizing the displacement of a massively dilated cecum away from the right lower quadrant (Fig. 8). Be-

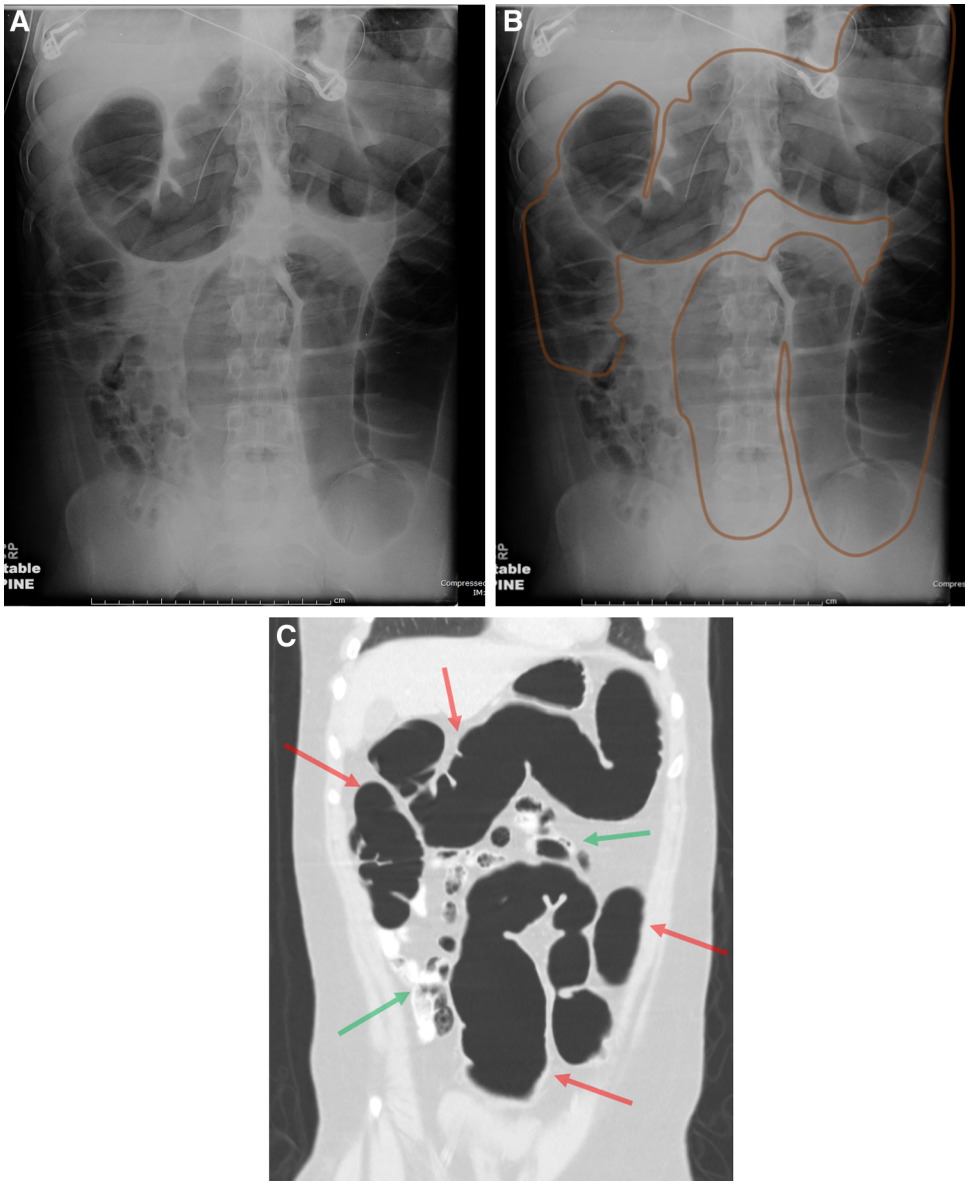

Fig. 9. **A** Abdominal radiograph demonstrating acute colonic pseudo-obstruction (ACPO). **B** Markedly dilated colon (*brown*) with no clear anatomical obstruction or transition point. **C** Coronal CT on lung windows demonstrating the diffusely dilated large bowel (*red arrows*) with normal small bowel (*green arrows*).

cause cecal volvulus is a relatively proximal LBO, the normal haustral markings of the colon are maintained and there is a greater chance of upstream small bowel dilatation—two features which are not entirely specific, but may help in differentiating cecal from sigmoid volvulus [27, 33].

Ogilvie syndrome or acute colonic pseudo-obstruction (ACPO), refers to the clinical picture of large bowel obstruction without any demonstrable evidence of actual mechanical obstruction [34]. Risk factors include medications that decrease motility, infection, recent surgery, and debilitation associated with severe medical or traumatic illness [35]. ACPO has a mortality rate as high as 40% should perforation occur, necessitating urgent attention once discovered [34]. In contrast to the typical radiographic appearance of a LBO described above, a pseudo-obstructed colon is massively dilated without any transition point or clearly evident obstructing lesion [36] (Fig. 9). Gas is usually present in the rectum, distinguishing ACPO from sigmoid volvulus. If ACPO is suspected, rectal gas may be more easily seen on a prone lateral or right lateral decubitus view [37].

Fecal impaction and constipation are frequently used synonymously, but are in fact separate diagnoses that are not mutually exclusive. Patients with constipation may experience painful and frustrating passage of hardened

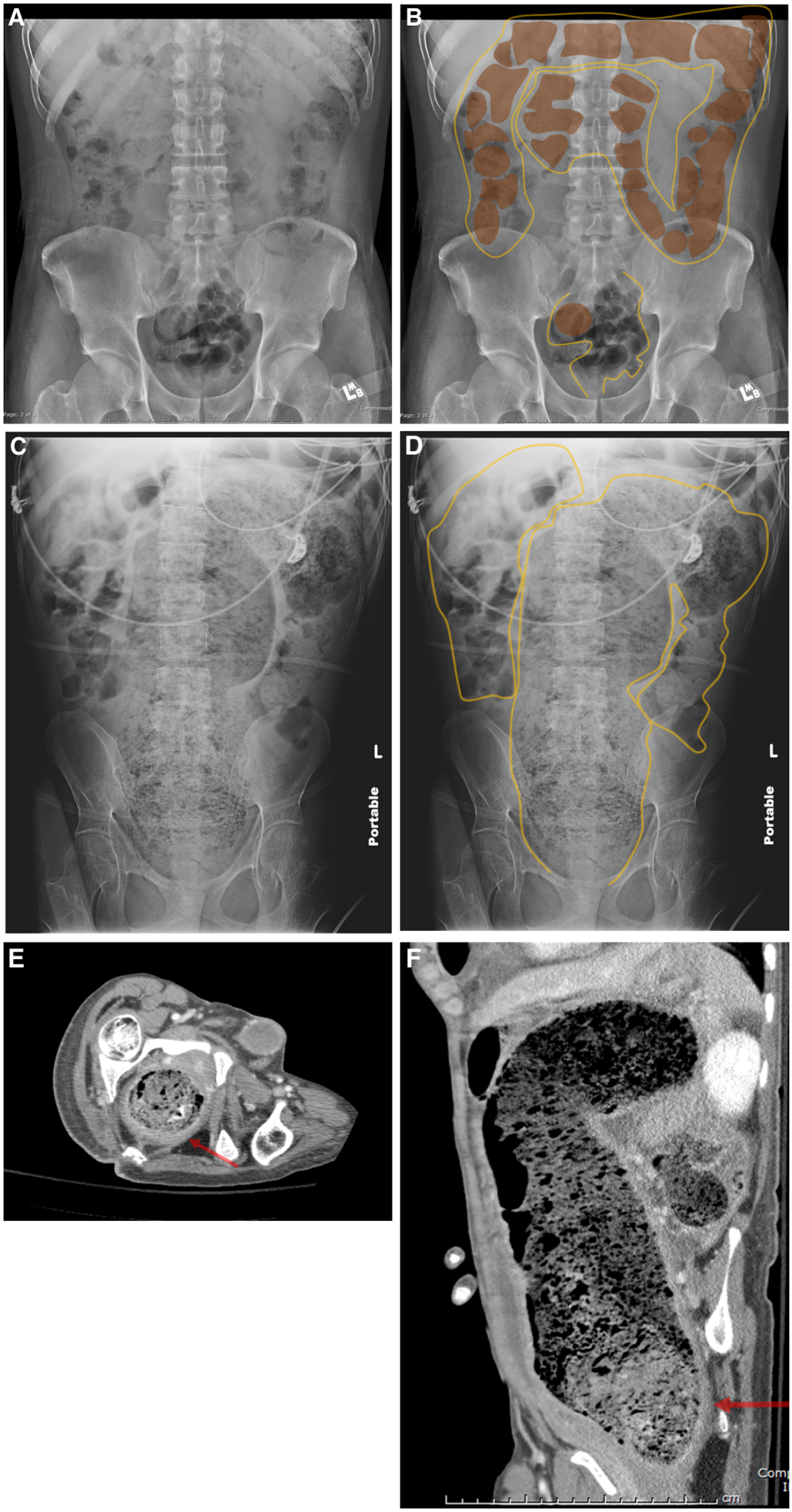

Fig. 10. **A** Abdominal radiograph demonstrating a large burden of feces distributed throughout the colon and rectum in a patient with a reported clinical history of constipation. **B** Copious feces (*brown*), large bowel lumen (*orange*). **C** Abdominal radiograph demonstrating an extreme case of fecal impaction. **D** Diffusely dilated colon (*orange*) filled with mottled feces. **E** Axial CT of the pelvis demonstrating bowel wall thickening in a dilated rectum filled with feces (*red arrow*). **F** Sagittal CT of the abdomen showing a massively dilated distal colon with wall thickening (*red arrow*).

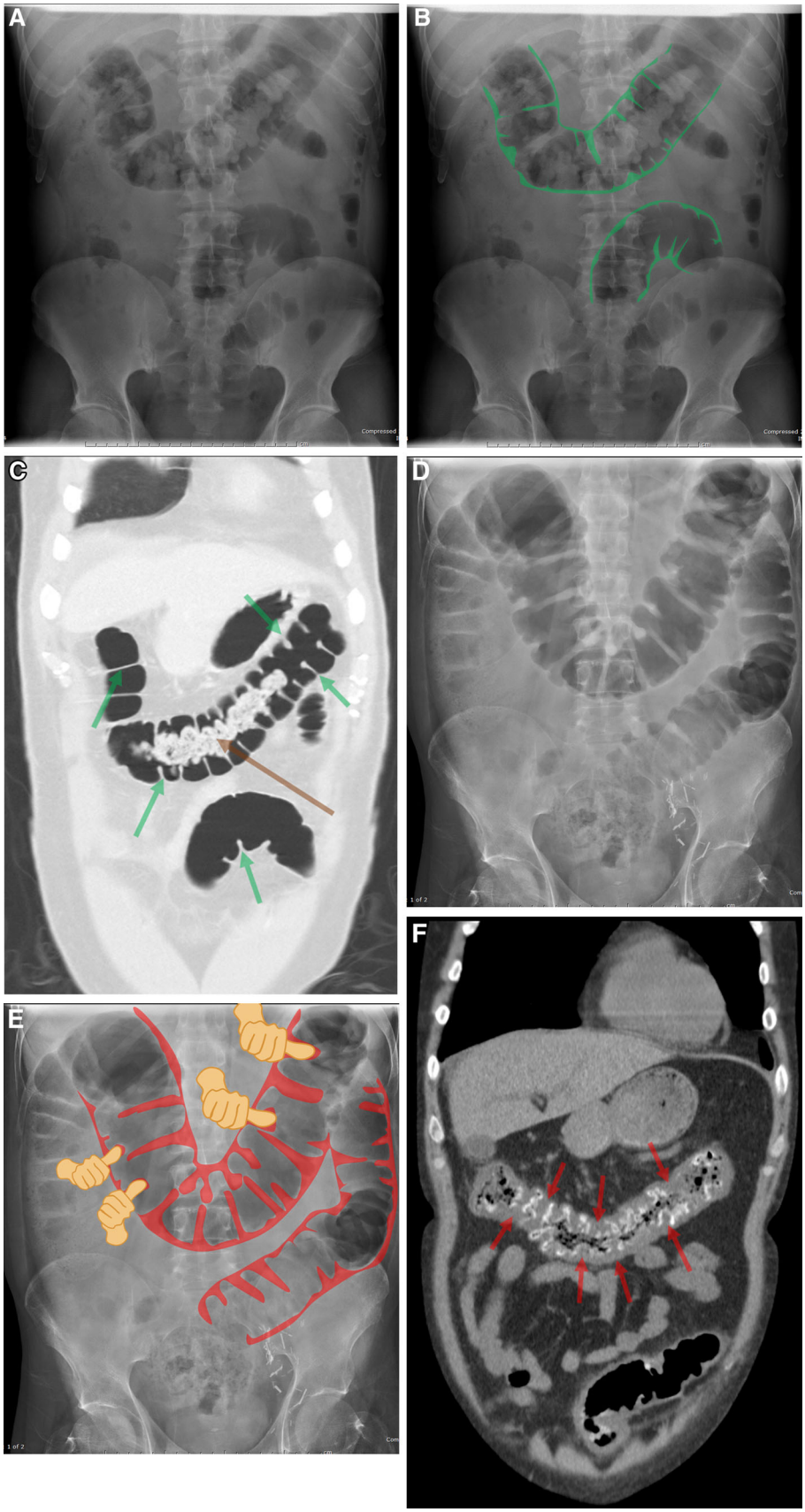

Fig. 11. **A** Abdominal radiograph demonstrating normal haustral folds. **B** Normal thickness of haustral folds (*green arrows*). **C** Coronal CT on lung windows demonstrating normal haustra (*green arrows*) in a colon with some feces (*brown arrow*). **D** Abdominal radiograph demonstrating classic "thumbprinting." **E** "Thumbprints" (*picture*) representing thickened haustral folds in the colon lumen (*red*). **F** Coronal CT of the abdomen showing diffuse colonic wall thickening and blunted haustra (*red arrows*).

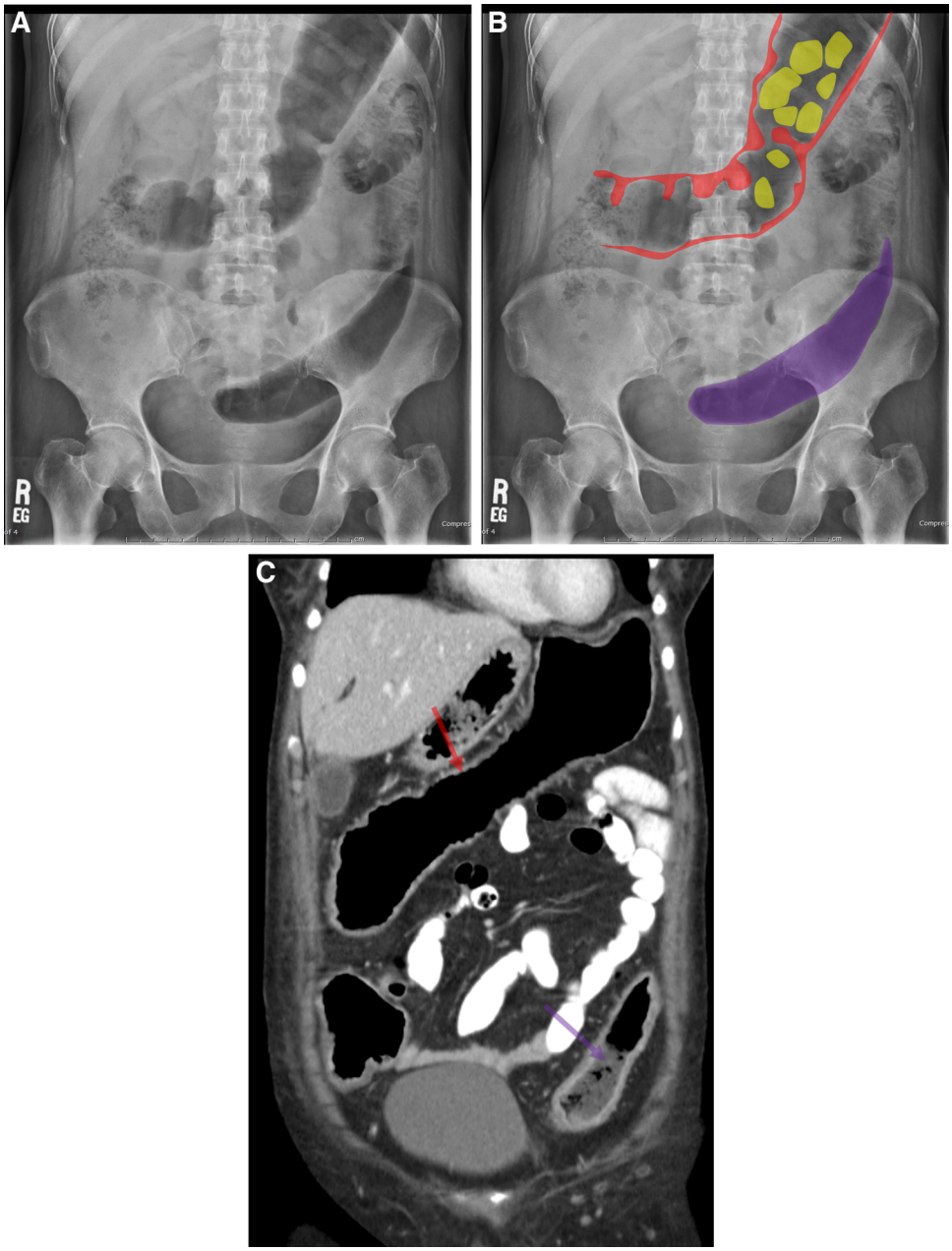

Fig. 12. **A** Abdominal radiograph demonstrating ulcerative colitis. **B** Decreased haustration with thickening of the remaining haustra (*red*), lead pipe colon (*purple*), classic edematous mucosal islands/pseudopolyps (*yellow*). **C** Coronal CT of the abdomen demonstrating diffuse colonic wall thickening with decreased haustration (*red arrow*), and a section of featureless lead pipe colon (*purple*).

stool in conjunction with the sensation of incomplete elimination. Constipation can still be present with normal stool frequency, defined as at least 3 bowel movements per week [38]. Fecal impaction typically refers to a large obstructing mass of hardened stool in the distal colon or rectum that may occur in the setting of constipation [39]. With regard to the radiologist, both entities are clinical diagnoses that cannot be made on imaging alone. However, fecal impaction is by far the most important diagnostic possibility to raise on abdominal plain film as it can lead to stercoral colitis and perforation if not promptly addressed. On plain film, fecal impaction is suggested by the presence of copious feces within a dilated segment of the colon >6 cm, most commonly at the distal sigmoid or rectum (Fig. 10). The feces may appear more dense than usual, reflecting a hardened and dehydrated state. When the degree of fecal impaction on plain film is subjectively severe with regards to the degree of colorectal dilatation and volume of feces, a CT scan should be recommended to exclude

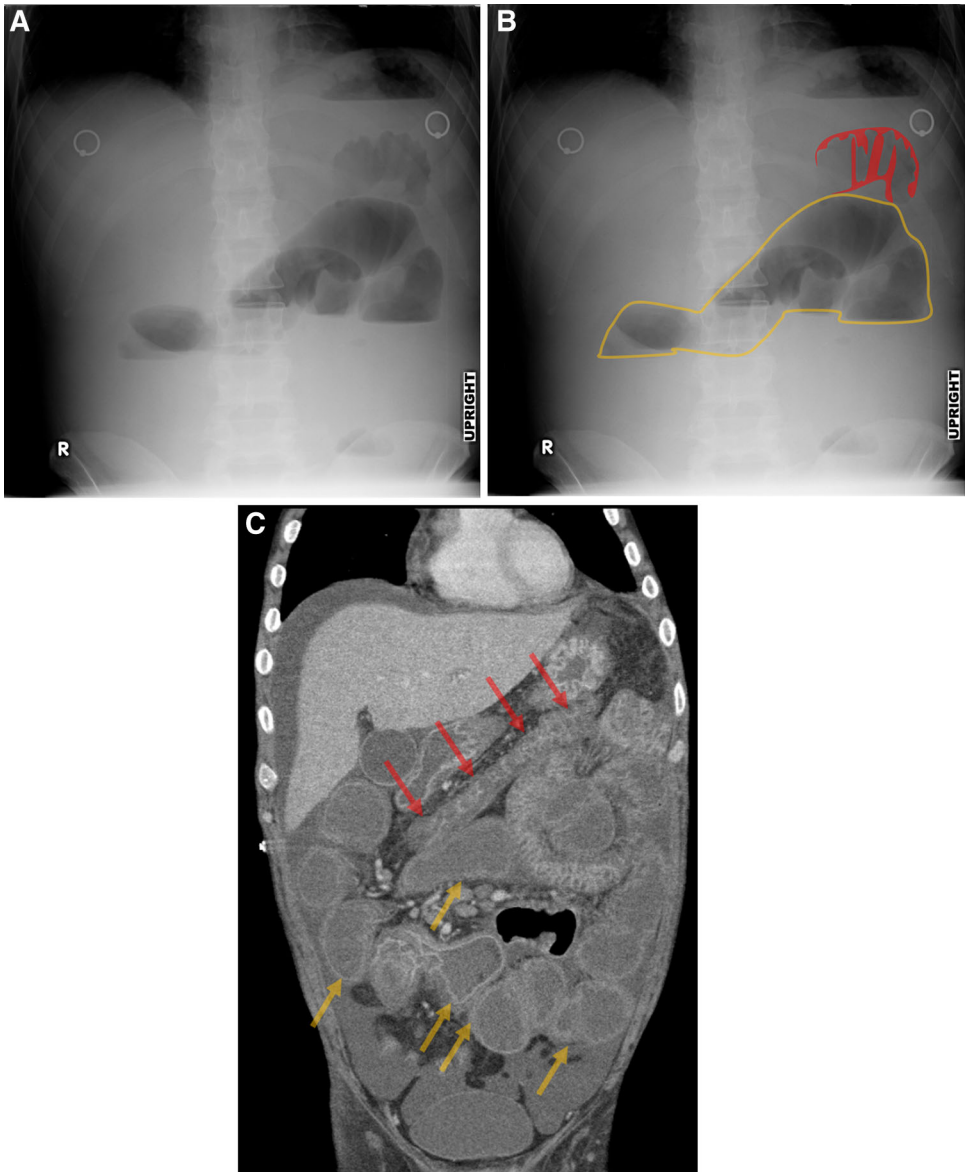

Fig. 13. **A** Abdominal radiograph demonstrating Crohn's disease. **B** Short segment of small bowel mural edema with thickening of the valvulae conniventes (*red*), dilated small bowel with multiple fluid levels concerning for obstruction (*orange*). **C** Coronal CT of the abdomen demonstrating mural thickening in a segment of small bowel in the *left upper* quadrant (*red arrow*). Fluid filled segments of distal small bowel with mural thickening (*orange arrows*).

stercoral ulcer or colitis. The presence of free air implies perforation and the need for immediate surgical attention [40]. On a final note regarding constipation in general, studies in both children and adults have demonstrated that the perceived amount of feces has wide interobserver variability and there is little correlation between the volume of feces and total colonic transit time (TCTT) [41, 42]. Instead of making the diagnosis of constipation, abdominal plain films are excellent at evaluating successful disimpaction—radiographs demonstrating decreased fecal burden correlated well with clinical response [41].

Normally, haustral folds are quite thin on plain film (Fig. 11), averaging only 3–4 mm in thickness. The plain film finding of "thumbprinting" pertains to the presence of thickened haustral folds, representing the bulbous impression of one's thumbprint [43]. These findings may be evident in inflammatory bowel disease, infectious colitis, intramural hematoma, and even lymphoma.

Beyond thumbprinting, a second stage of haustral devolution occurs with ulcerative colitis (UC), where there is complete loss of normal haustration, termed a "lead pipe" or "featureless" colon (Fig. 12). Presumably, this is due to alterations in muscle tone of the teniae coli

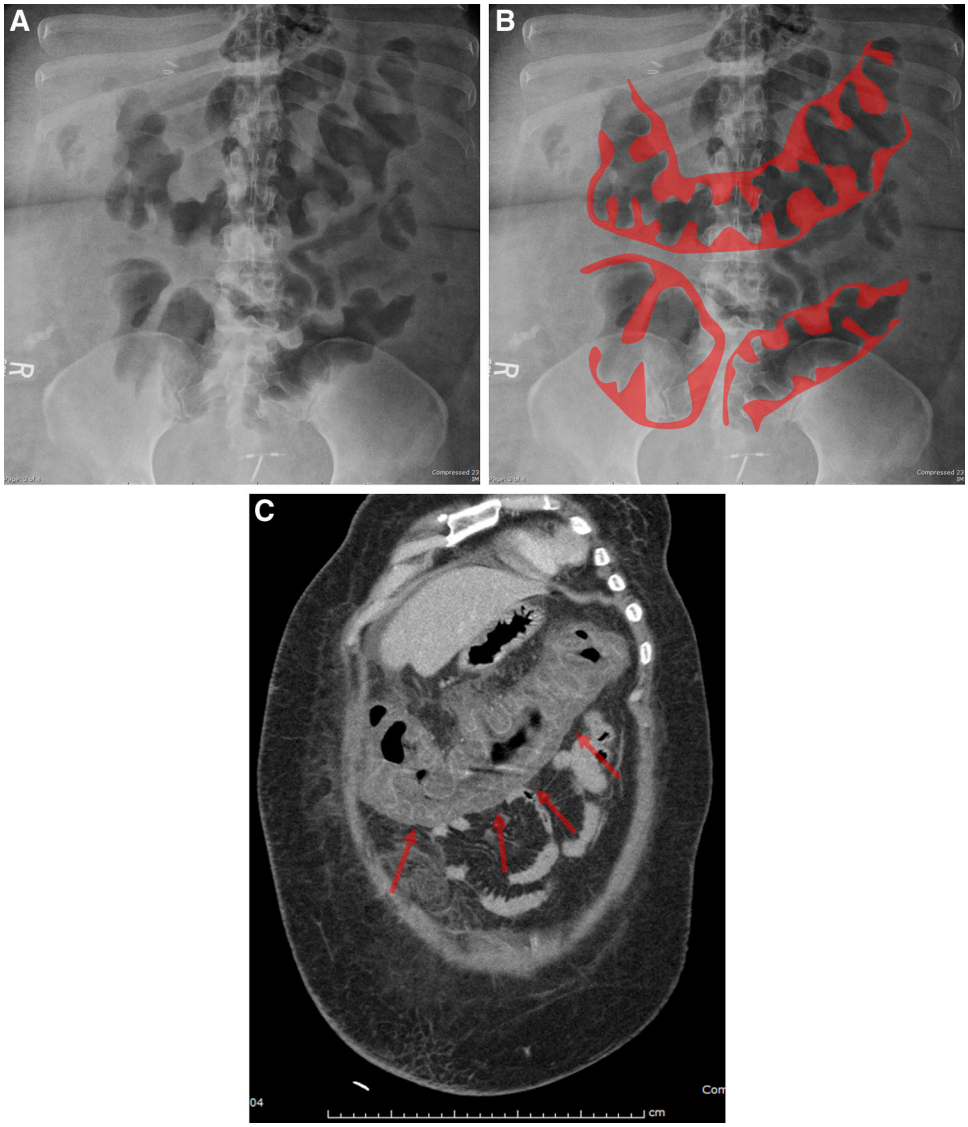

Fig. 14. **A** Abdominal radiograph demonstrating pseudomembranous colitis. **B** Extensive nodular thumbprinting representing diffuse haustral and colonic thickening seen in the cecum, transverse, and sigmoid colon (*red*). **C** Coronal CT of the abdomen showing diffuse transverse colon colitis (*red arrows*).

from the chronic inflammation. The lead pipe colon reflects burned-out disease and is not a good reflection of active disease. Ill-defined patchy islands of soft tissue density overlying the distended large bowel can be seen, representing pseudopolyps. Pseudopolyps are the remnant islands of inflamed mucosa that persist following extensive ulceration seen with severe UC [44]. Abdominal plain film has some utility in evaluating UC because severe disease brings about an increase in gas throughout the intestines. This increased gas enhances detection of UC findings because adequate distention aids the evaluation of mucosal pathology. Irregularity of the mucosal edge and increased wall thickness are most predictive of lesion extent. Wall thickness of 3–4 mm is common with chronic and subacute UC while thickening >8 mm suggests more severe colitis [45].

An analogous finding to thumbprinting may be seen in the small bowel with Crohn's disease. The presence of small bowel wall thickening on plain film can help differentiate Crohn's disease from UC, since the latter does not involve the small bowel. In contrast to large bowel thumbprinting, small bowel mural thickening will present as comparatively smaller mucosal invaginations obscuring the normal valvulae conniventes (Fig. 13). There will also be apparent increase in the thickness of the soft tissue between adjacent bowel segments reflecting mural edema [46]. Furthermore, the presence of intermittent segments of thumbprinting or small bowel

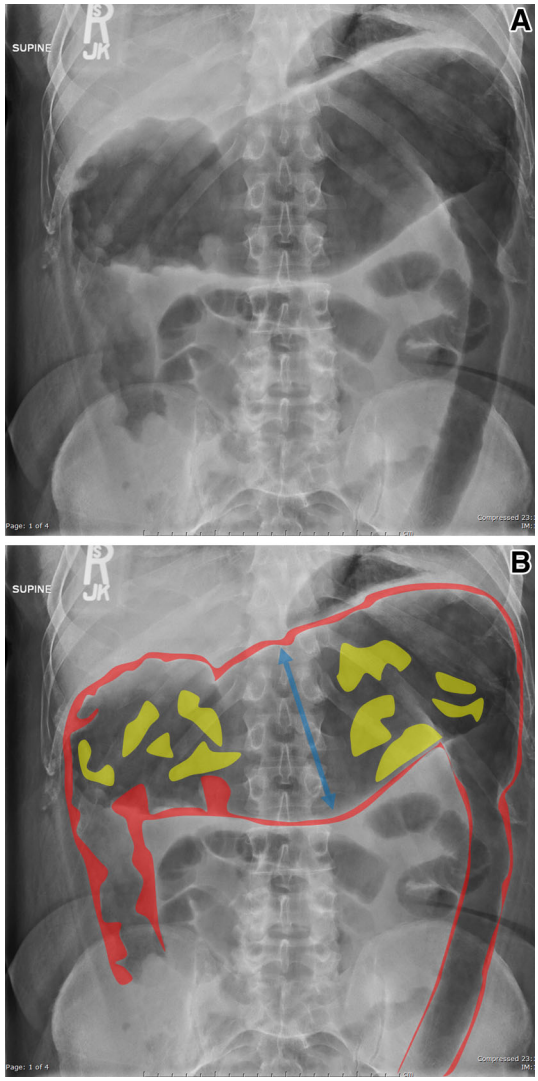

Fig. 15. **A** Abdominal radiograph demonstrating toxic megacolon in the setting of UC. **B** Massive transverse colon dilatation (*blue double arrow*); decreased haustration with a featureless "lead pipe" descending colon (*red*); irregular mucosa and pseudopolyps (*yellow*).

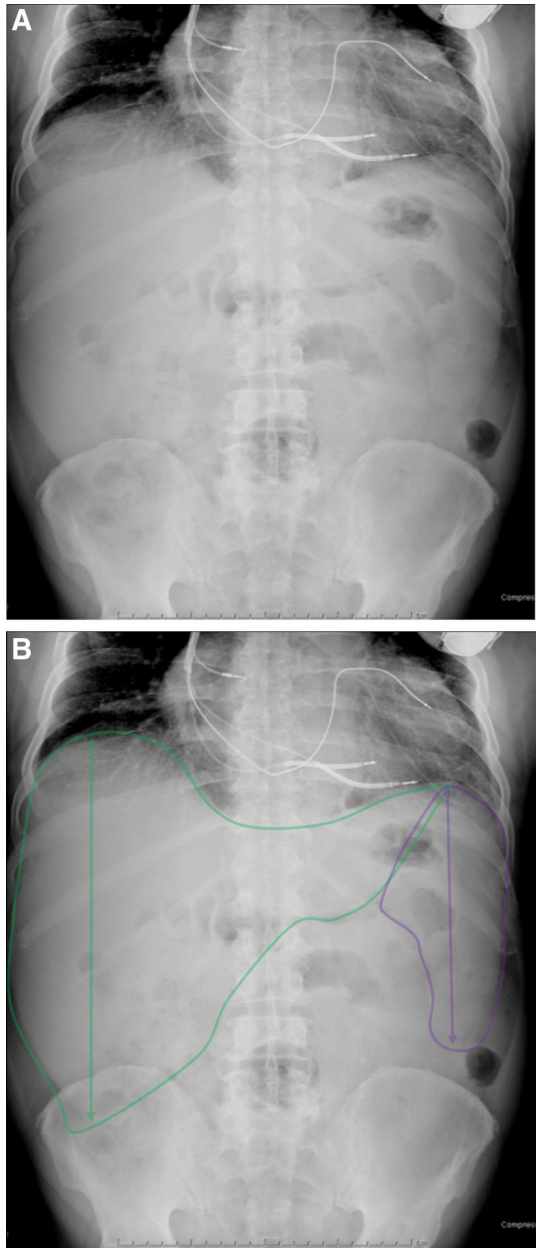

Fig. 16. **A** Abdominal radiograph demonstrating hepatosplenomegaly. **B** Enlarged liver (*green*), enlarged spleen (*purple*).

mural thickening interrupted by normal mucosal pattern may suggest the presence of skip lesions, favoring a diagnosis of Crohn's disease. Despite these characteristic plain film findings, the vast majority of plain films in Crohn's disease are normal. The findings described are neither sensitive nor specific enough to have a significant impact on clinical management in the ED [46].

Pseudomembranous colitis (PMC) may demonstrate more nodular haustral thickening in addition to the thumbprinting described above, representing the characteristic "pseudomembranes" seen on gross pathology (Fig. 14). Secondary plain film signs include ileus and ascites. Given the wide range of disease severity, abdominal plain film findings can suggest the diagnosis but are neither very sensitive nor specific [47].

Toxic megacolon is a life-threatening condition characterized by severe dilatation of the large bowel without obstruction in the clinical setting of system toxicity (fever, tachycardia, leukocytosis), most commonly from infectious or inflammatory disease. Typi-

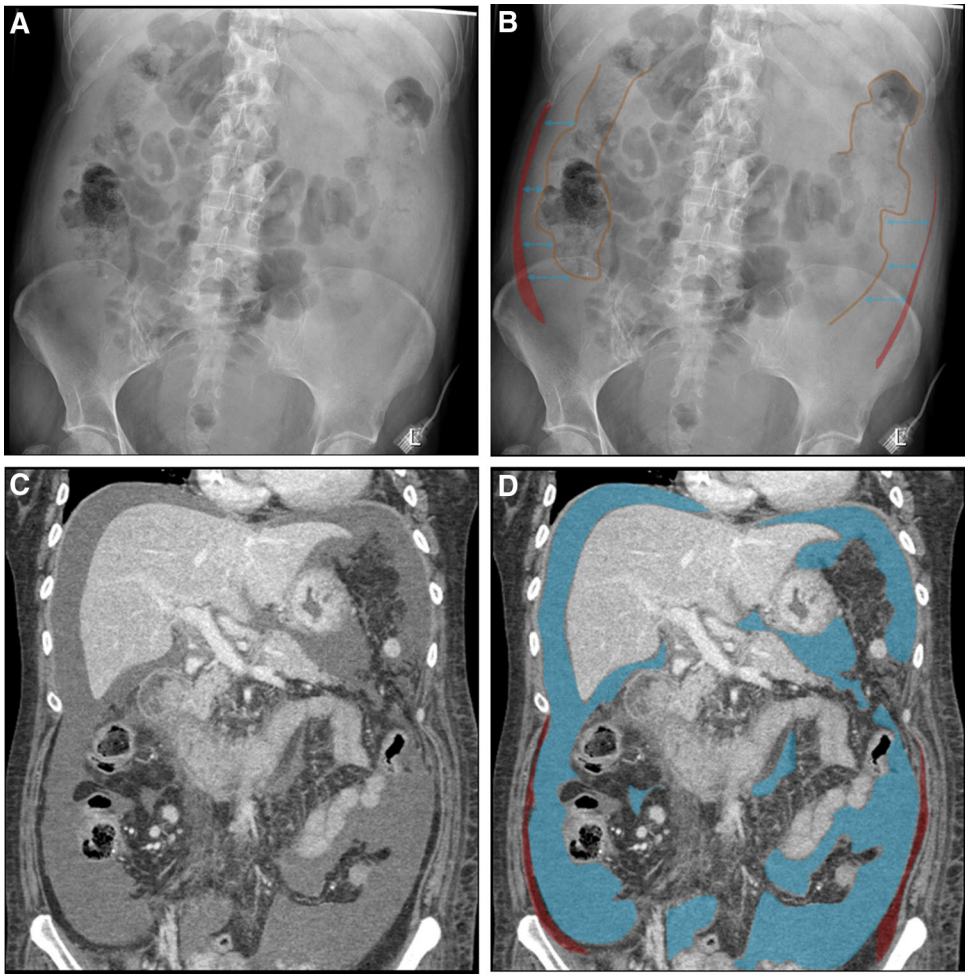

Fig. 17. **A** Abdominal radiograph demonstrating ascites with displacement of bowel loops centrally. **B** Ascites (*blue*), large bowel (*brown*), preperitoneal fat stripe (*red*). **C** Coronal CT abdomen and pelvis with moderate ascites. **D** Ascites (*blue*), preperitoneal fat stripe (*red*).

cally, the transverse colon is dilated up to at least 6 cm; studies have shown a mean colonic diameter of 9.2 cm [48]. There will likely be additional plain film signs such as thumbprinting, pseudopolyps and loss of haustral folds (Fig. 15). A clinical history of UC or PMC should raise one's suspicion for toxic megacolon in the setting of massive large bowel dilatation. Abdominal plain film is valuable to determine the presence of free air, which implies perforation and necessitates urgent surgical intervention.

Abdominal organs

Common findings on abdominal radiograph include organomegaly, as well as loss of normal intraperitoneal fat planes, as seen in ascites.

Hepatomegaly can occur as a result of infection, portal or systemic venous hypertension, or congenital metabolic disease [49]. Hepatomegaly is defined as liver size >17 cm [50]. Splenomegaly is defined as a spleen size >13 cm, and can be associated with infections, liver disease, anemia, and hematologic malignancy [51]. Hepatomegaly and splenomegaly can be found in isolation, but are frequently seen together in the setting of chronic liver disease [49]. On plain film, an enlarged liver and spleen are seen by training one's eye to find the fat planes and follow the large area of increased soft tissue density in the right and left upper quadrants (Fig. 16). To see the organ borders, start laterally along the ribs and follow the line between the high density of the organ and low density of the mesenteric fat at it curves along the inferior tip of the organs and back up again. The digital measurement scale can be used, or if there is doubt regarding appropriate correction factor, the average size of a lower thoracic/lumbar vertebrae (2.5 cm) can be used as a scale [52].

Ascites is the accumulation of fluid in the peritoneal cavity, which can result from many processes including systemic venous hypertension, intra-abdominal malignancy, or serositis [49]. On supine plain film, ascites can

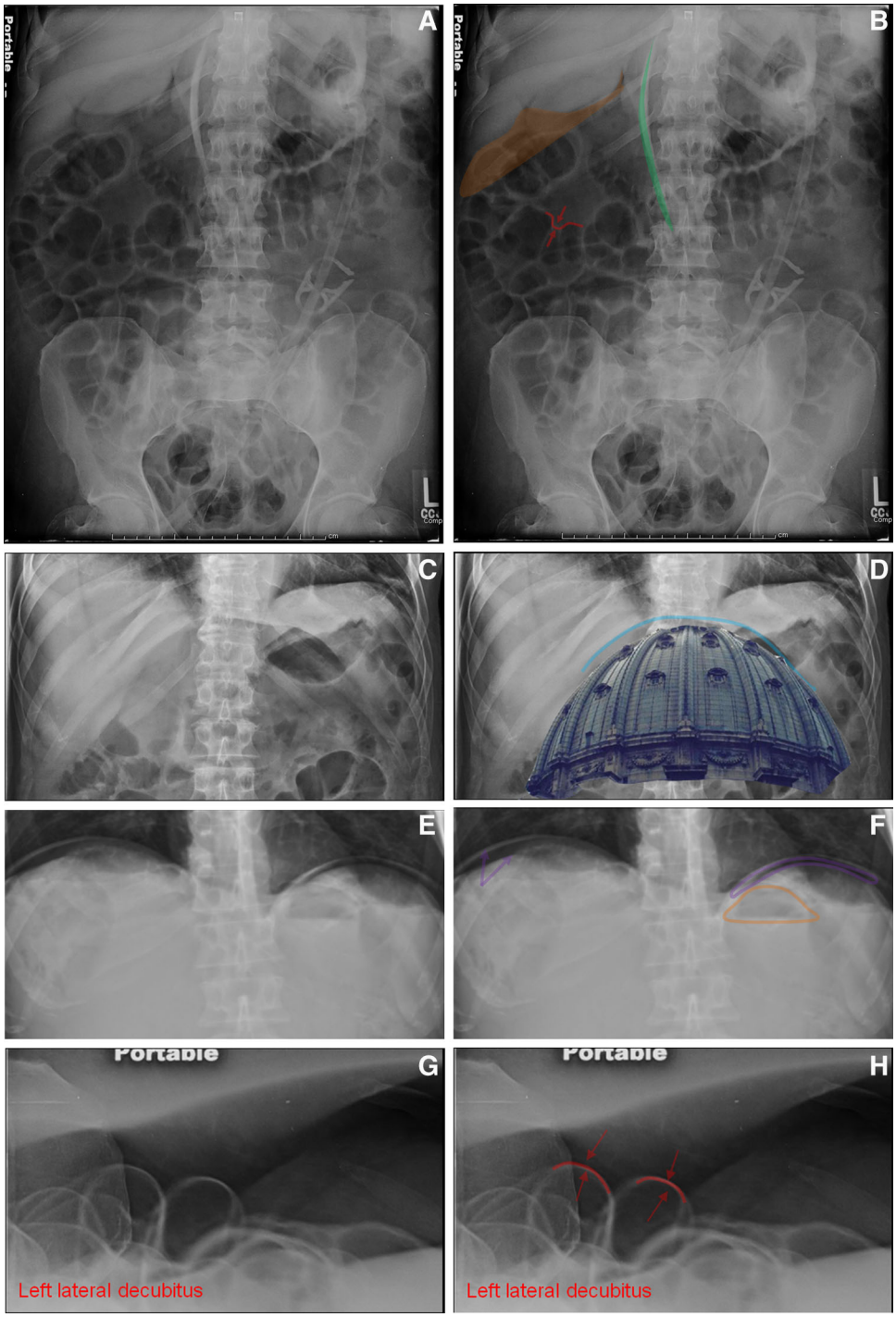

Fig. 18. Examples of free air. **A** Abdominal radiograph demonstrating massive free intraperitoneal air. **B** Air anterior to ventral liver (*brown*), Rigler's sign (*red*), falciform ligament sign (*green*). **C** Free air with the Cupola Sign. **D** Cupola sign (*overlay*). **E** Double bubble sign. **F** Double bubble sign, with gas below the diaphragm (*purple*), and normal stomach bubble (*orange*). **G** Left lateral decubitus view with free air. **H** Rigler's sign (*red*) on left lateral decubitus radiograph.

present as diffusely increased hazy density of the abdomen and centralized displacement of bowel loops away from the preperitoneal fat stripe with bulging flanks (Fig. 17). Normal soft tissue silhouettes of the liver, spleen, and psoas muscles may not be well seen due to the surrounding fluid, which results in loss of normal intraperitoneal fat planes [53].

Pathologic gas

Pathologic gas can present on abdominal radiograph in myriad forms, including pneumoperitoneum, pneumatosis, portal venous gas, and emphysematous pyelonephritis or cystitis. Extra-abdominal gas, as in pneumothorax, may also be seen.

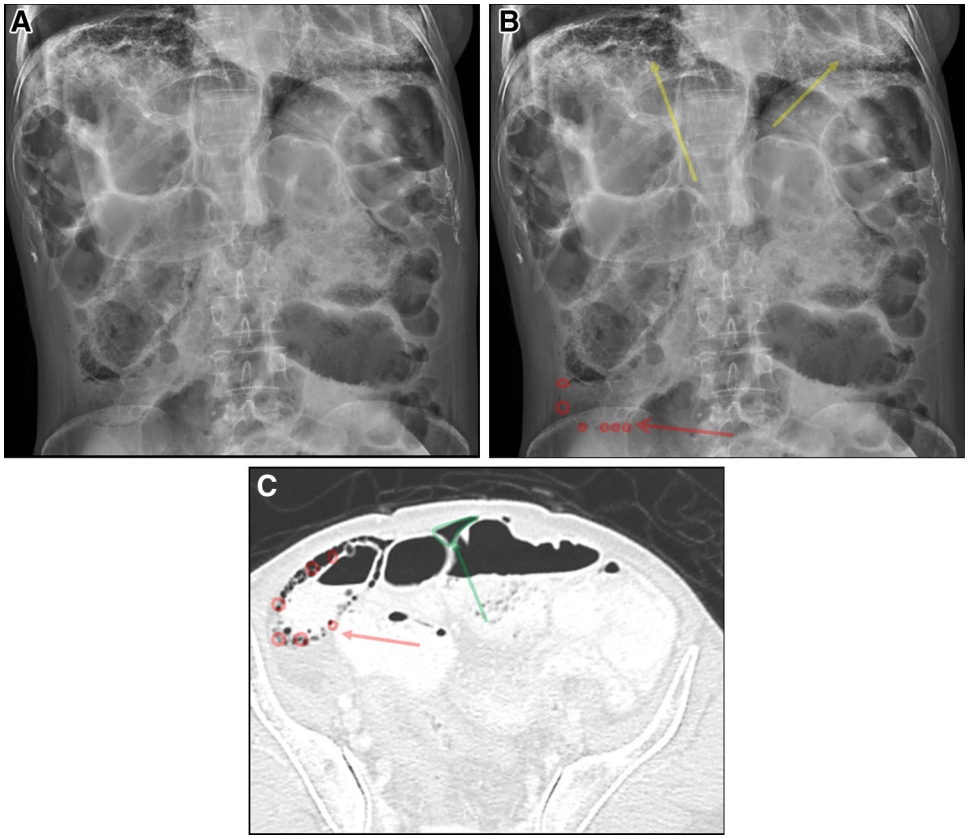

Fig. 19. **A** Abdominal radiograph in patient with scleroderma demonstrating bowel pneumatosis. **B** Bowel wall pneumatosis (*red*). Fibrosis of the lung (*yellow*). **C** Axial CT on lung windows at the level of the pelvis showing unchanged bowel pneumatosis (*red*) in a patient with sclerodema. A small collection of extraluminal gas is also seen (*green*).

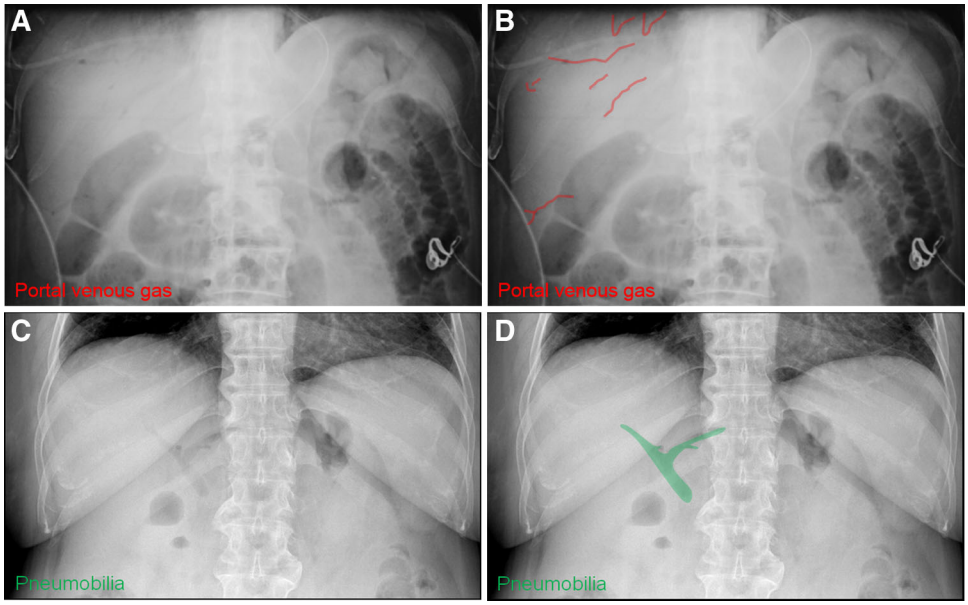

Fig. 20. **A** Abdominal radiograph demonstrating portal venous gas. **B** Outlined peripheral, branching lucency representing portal venous gas (*red*). **C** Pneumobilia. **D** Outlined central lucency representing pneumobilia (*green*).

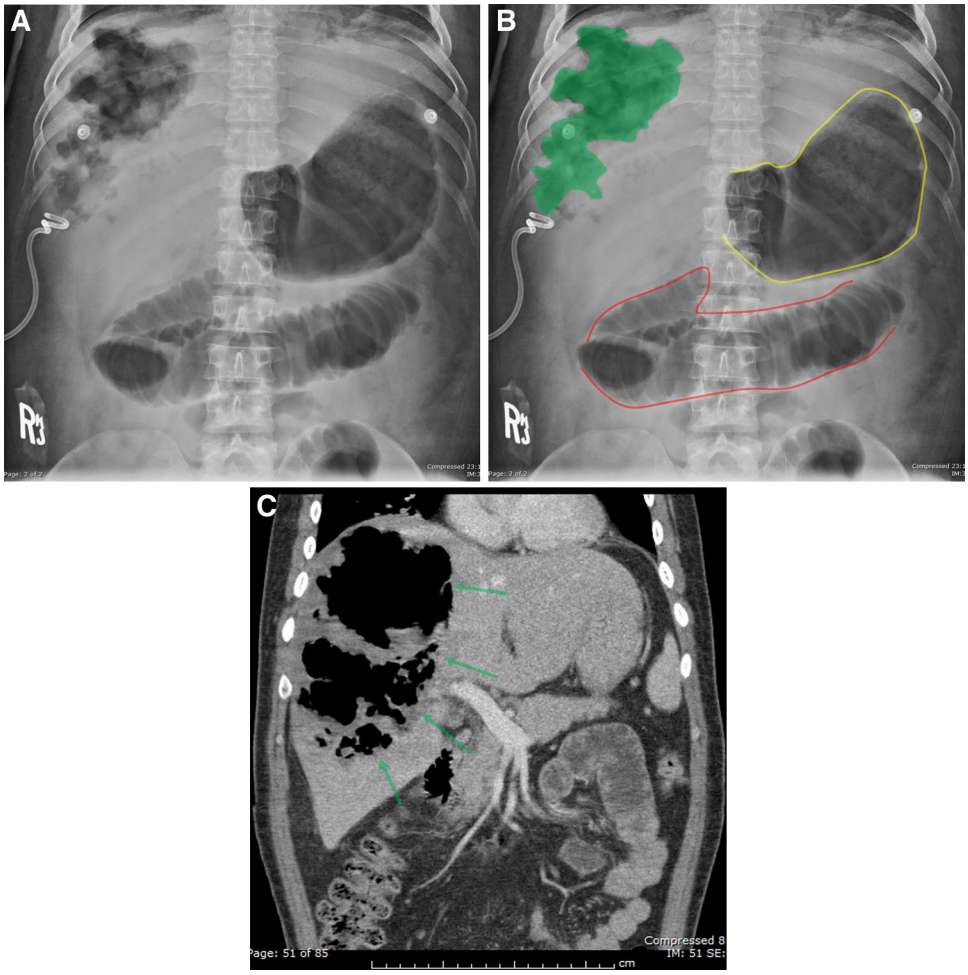

Fig. 21. **A** Abdominal radiograph demonstrating a hepatic abscess. **B** Large cavity within the right hepatic lobe (*green*), distended stomach (*yellow*), focal small bowel ileus (*red*). **C** Coronal CT abdomen showing a large, irregular cavitation within the right hepatic lobe (*green arrows*).

Pneumoperitoneum is the accumulation of air within the peritoneal cavity, which can result from bowel perforation or iatrogenic cause [54]. Following abdominal surgery, pneumoperitoneum is a frequent finding, and can be seen as long as several weeks postoperatively [55]. On the other hand, unexpected pneumoperitoneum, in the absence of recent surgery or intervention, is often a surgical emergency warranting immediate notification of the primary physician. Common imaging signs of pneumoperitoneum (Fig. 18) include

1. Rigler's—visualization of air on both sides of the bowel wall
2. Falciform—appearance of a linear opacity from the liver to the mid abdomen
3. Cupola—air beneath the central tendon of the diaphragm
4. Double bubble—subdiaphragmatic gas outlining the wall of stomach and diaphragm
5. Air anterior to ventral liver—geographical lucency over the liver silhouette

Bowel wall pneumatosis can occur in numerous conditions, both benign and pathologic. Common etiologies include ischemia, iatrogenic, chronic obstructive pulmonary disease (COPD), chemotherapy, collagen-vascular diseases, and Whipple disease [56]. On plain film, there may be a mottled appearance of the bowel wall which is difficult to distinguish from stool. The concomitant presence of gas in the portal circulation is suspicious for bowel ischemia [57]. Pneumatosis itself is not a specific radiographic finding; for example, scleroderma is a frequent cause. In the example shown, multiple CT scans showed unchanging bowel pneumatosis

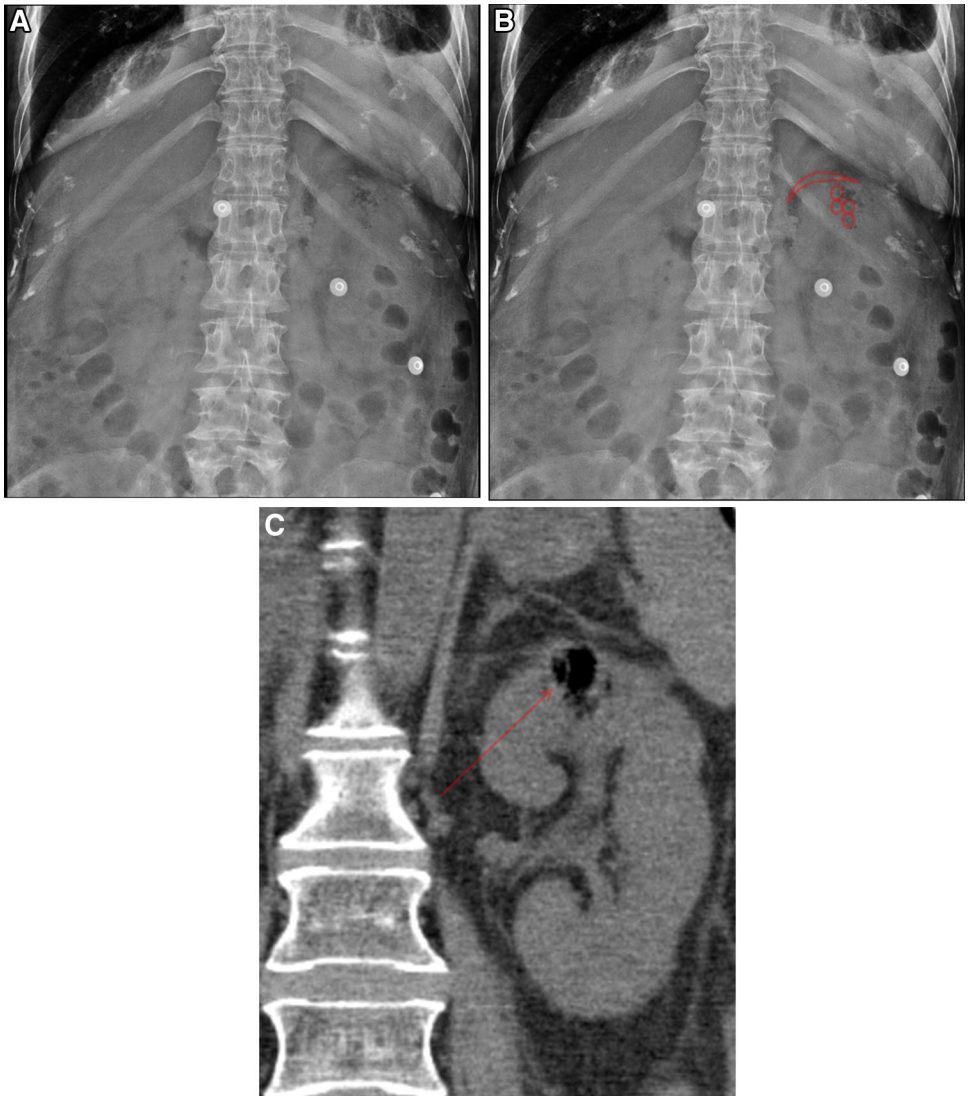

Fig. 22. **A** Abdominal radiograph demonstrating emphysematous pyelonephritis. **B** Gas overlying the renal parenchyma and also along the perinephric space (*red*). **C** Coronal CT abdomen on bone windows showing gas (*red arrow*) within the upper pole of the left kidney.

with persistent benign pneumoperitoneum over several months. Pulmonary fibrosis in the superior aspect of the abdominal radiograph was consistent with the diagnosis of scleroderma (Fig. 19).

Portal venous gas can be seen in bowel ischemia. Other causes, both benign and pathologic, include necrotizing enterocolitis (NEC) in children, iatrogenic following bowel surgery or endoscopy, inflammatory bowel disease, and COPD [58]. On plain film, portal venous gas manifests as serpiginous and linear lucencies over the liver, which should be differentiated from pneumobilia (Fig. 20). Pneumobilia appears more centrally, while portal venous gas is finer and more peripheral [59].

Gas overlying the right upper quadrant should be carefully evaluated for hepatic abscess or emphysematous cholecystitis and distinguished from colonic or duodenal gas [60]. A large irregular collection of gas over the liver would favor a hepatic abscess (Fig. 21). The evolution of the plain film gas pattern in emphysematous cholecystitis follows three stages: (1) intraluminal gas within 48 h of symptoms, (2) intramural gas demonstrated by ring or crescentic lucency outlining the gallbladder, (3) perforation and abscess producing a mottled

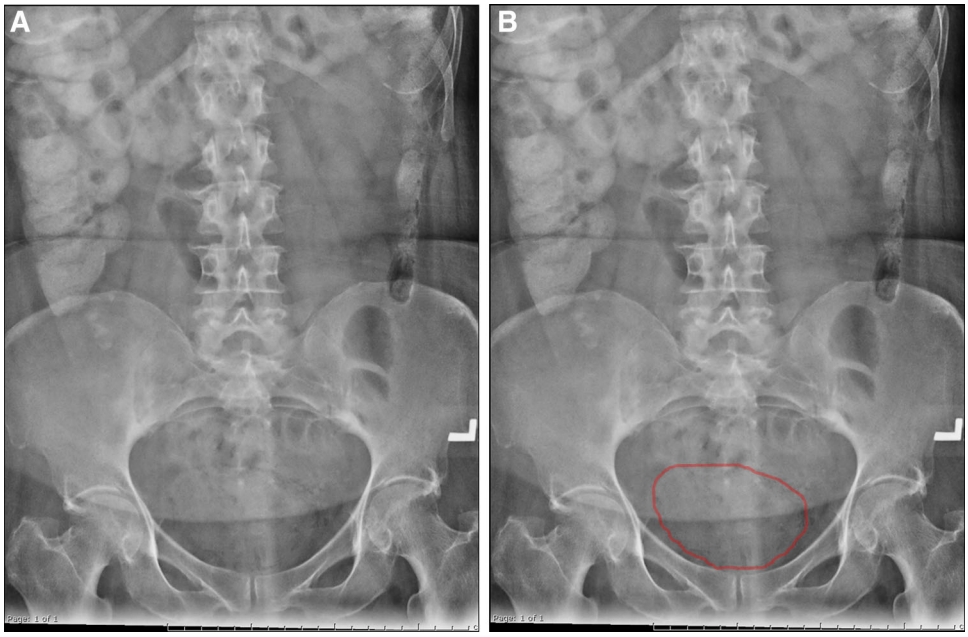

Fig. 23. **A** Abdominal radiograph demonstrating emphysematous cystitis. **B** Gas outlining the bladder wall (*red*).

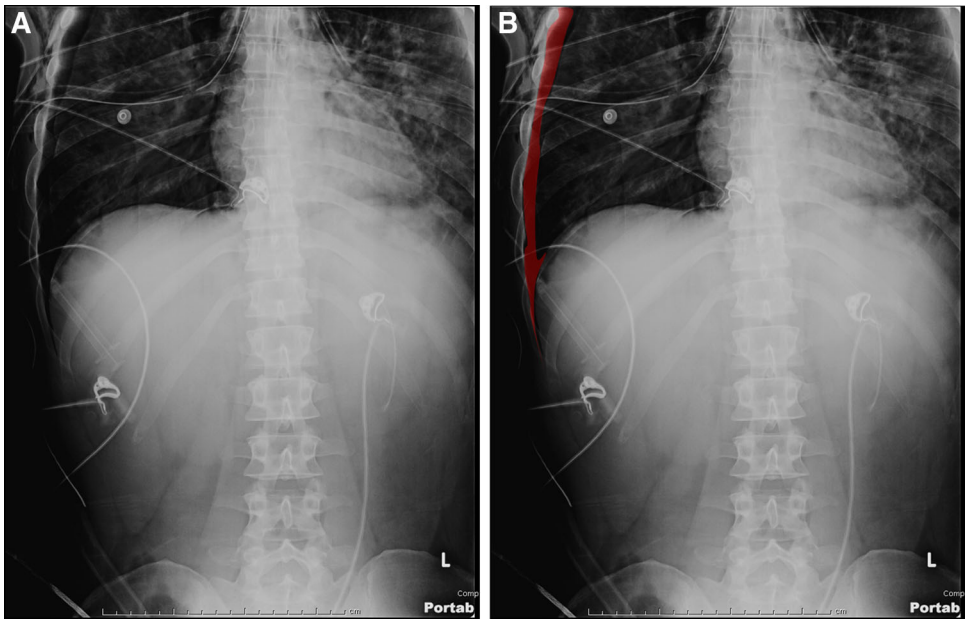

Fig. 24. **A** Abdominal radiograph demonstrating right-sided pneumothorax. **B** Gas within the right lateral pleural space (*red*).

gas collection in the right upper quadrant, which is very difficult to differentiate from a hepatic abscess on plain film. A rare finding pathognomonic of emphysematous cholecystitis is gas surrounding intraluminal calculi on multiple projections.

Emphysematous pyelonephritis is a severe infection of the kidneys with fulminant course, usually caused by *E. coli or Klebsiella* spp. Diabetes is a major risk factor for development. On plain film, the diagnosis can be made by identifying streaky, mottled, or bubbly lucencies representing gas from bacterial fermentation overlying the renal parenchyma (Fig. 22). Some studies suggest that the parenchymal gas pattern (streaky versus bubbly) and the presence or lack of a fluid collection may be

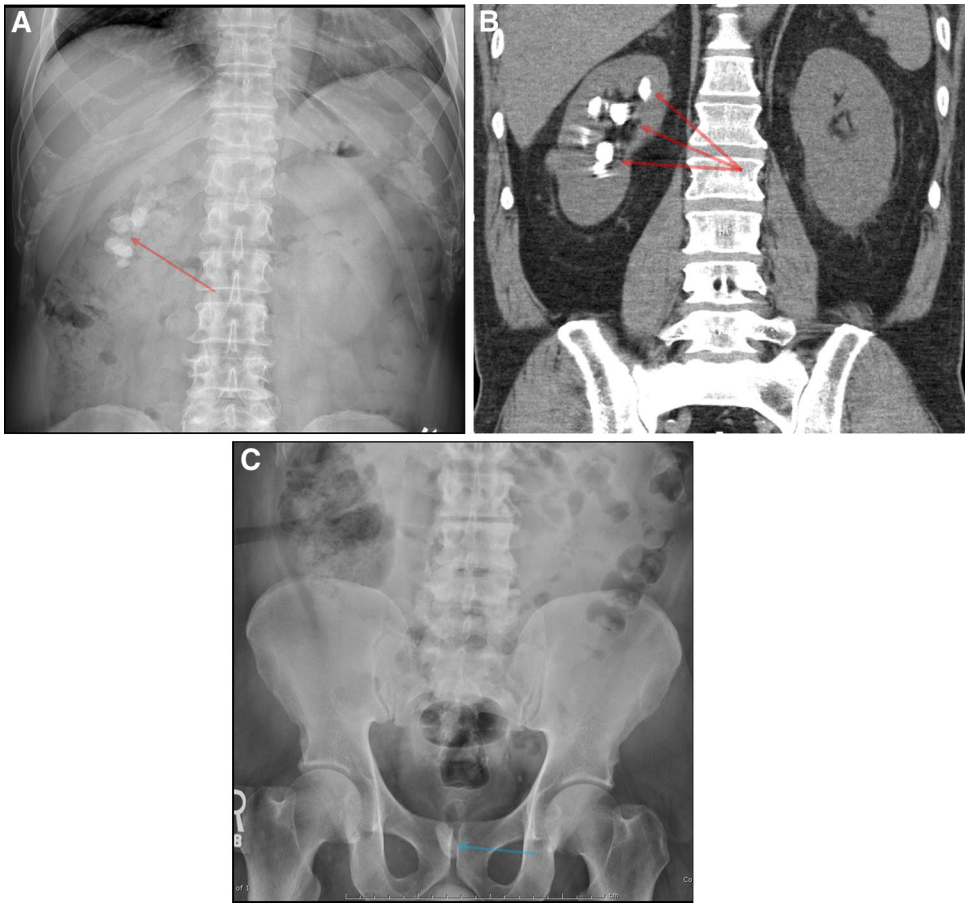

Fig. 25. **A** Abdominal radiograph demonstrating nephrolithiasis (*red arrow*). **B** Coronal noncontrast CT on soft tissue windows showing multiple renal stones within the calyces (*red arrows*). **C** Bladder stone projecting over the pubic symphysis (*blue arrow*).

prognostic factors. Bubbly gas and fluid collections are thought to be favorable and predict a less fulminant course of disease (emphysematous pyelitis rather than true pyelonephritis), but CT is more reliable for detailed evaluation [61]. Care must be taken not to confuse bowel gas with renal parenchymal gas as they can sometimes be very difficult to differentiate. Concentric rings of lucency around the renal silhouette imply involvement of the perinephric space. If the ureter is obstructed, gas within the calyces and collecting system may be seen [62]. Emphysematous pyelonephritis is typically encountered in critically ill patients, and may require emergent percutaneous drainage or nephrectomy [63].

Emphysematous cystitis is a complicated infection of the bladder, typically seen in diabetic patients. As with emphysematous pyelonephritis, *E. coli or Klebsiella* spp. are the most common pathogens. Unlike emphysematous pyelonephritis, which has a high associated morbidity, emphysematous cystitis has a benign course and is managed by urethral catheter and antibiotics [64]. On plain film, lucent gas can be seen within the bladder wall (Fig. 23).

A pneumothorax is a collection of gas or air within the pleural space. It can result from trauma, iatrogenic cause, or even be spontaneous. Large pneumothoraces can compromise respiratory function and may require decompression by a chest tube. On plain film, lucent gas can be seen outlining the pleura and separating it from the chest wall. On a supine abdominal film, a "deep sulcus" sign can be seen, characterized by air collecting in the costophrenic angle, increasing the separation between the diaphragm and chest wall (Fig. 24) [65].

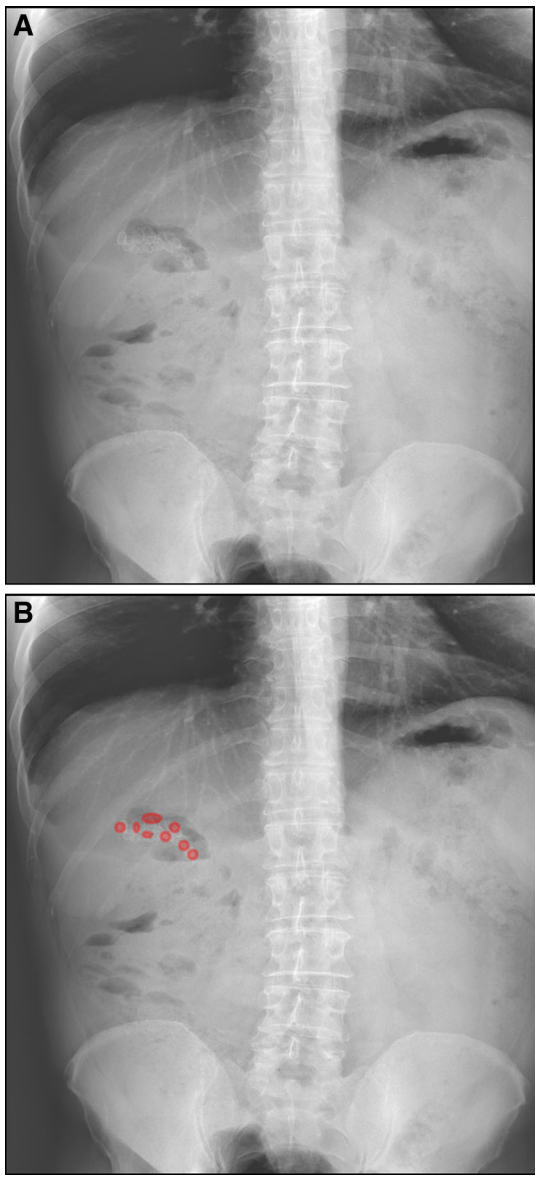

Fig. 26. **A** Abdominal radiograph demonstrating cholelithiasis. **B** Multifaceted calcifications in the *right upper* quadrant in the expected shape of a gallbladder lumen (*red*).

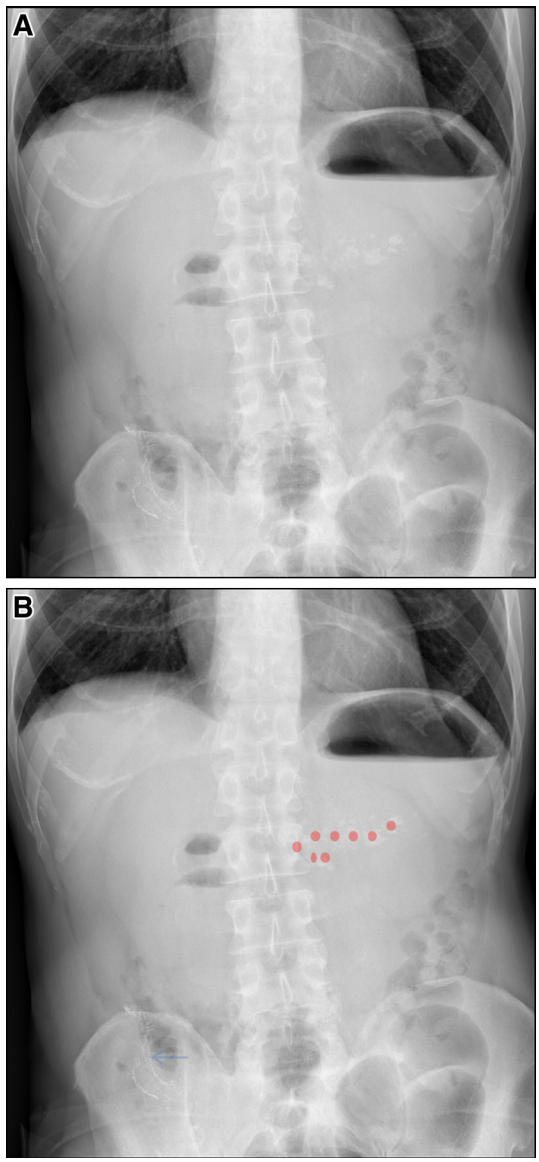

Fig. 27. **A** Abdominal radiograph demonstrating chronic pancreatitis. **B** Multiple small irregular calcifications over the expected region of the pancreas (*red*), Incidental bowel anastomosis suture (*blue arrow*).

Calcifications

Calcifications can be seen on abdominal radiograph in conditions including urolithiasis and cholelithiasis. Calcifications can also be a manifestation of prior infection or inflammation, as in chronic pancreatitis, calcified lymph nodes, and atherosclerotic vascular disease.

Urolithiasis is the formation of calculi in the urinary tract. The clinical pattern of pain can suggest the stone's location. For example, stones at the ureteropelvic junction will cause deep flank pain, without radiation to the groin. Ureteral stones will cause severe ipsilateral pain with radiation to the groin. Bladder stones are typically asymptomatic. On plain film, urinary tract stones can appear as calcifications that overly the kidneys, bladder, or the expected path of the ureters (Fig. 25). The sensitivity of radiographs for detecting urolithiasis is lower than that of CT (59% versus 97%) [66]. Making a specific

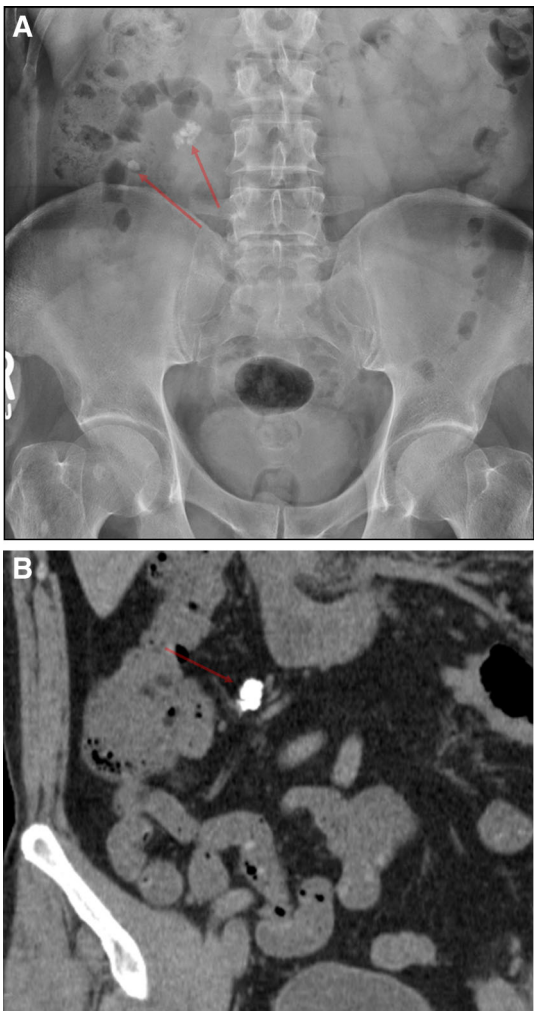

Fig. 28. **A** Abdominal radiograph demonstrating calcified lymph nodes in the *right lower* quadrant (*red arrows*). **B** Coronal CT on soft tissue windows demonstrating that the plain film *right lower* quadrant calcification is a lymph node adjacent to mesenteric vessels (*red arrow*).

diagnosis of urolithiasis on plain film is also challenging, in large part because phleboliths (venous calcifications) are common in the pelvis. A lucent center is a common finding of phleboliths on plain film which can help to differentiate them from urolithiasis [67]. The radiographic visibility of stones varies depending on composition; calcium-based stones are radiodense, while uric acid stones are radiolucent and cannot be seen on plain film [68].

Cholelithiasis is the presence of calculi within the gallbladder lumen. While gallstones may be asymptomatic, obstruction of the biliary tree by stones can cause severe pain and gallbladder inflammation. On plain film, right upper quadrant lamellate and multifaceted calcifications can be seen (Fig. 26). Only 15% of gallstones contain enough calcium to be visible on abdominal radiographs; cholesterol predominant stones are far more prevalent [69].

Chronic pancreatitis is defined as long-standing inflammation of the pancreas that leads to decreased function and structural deformity of the organ. Patients may have persistent pain and steatorrhea, leading to weight loss and malnutrition [70]. On plain film, small, irregular and diffuse calcifications are seen over the expected location of the pancreas in the mid-abdomen (Fig. 27) [71].

Calcified lymph nodes are common, and are usually the sequela of prior granulomatous disease such as tuberculosis. On plain film, calcified mesenteric lymph nodes can be difficult to distinguish from urolithiasis, especially when overlying the kidneys or ureters (Fig. 28). However, a large cluster of calcifications or a relatively lateral position suggests lymph nodes [72].

Although not always seen in cases of acute appendicitis, an appendicolith can be a fortuitous finding on abdominal plain film and presents as an ovoid, often lamellar calcified body in the right lower quadrant (Fig. 29). Lamella may help differentiate an appendicolith from calcified lymph nodes, bone islands, phleboliths, and pills. They are present on plain film in 2%–15% of all cases of appendicitis. The specificity of a suspected appendicolith for appendicitis can reach about 94% [3]. Furthermore, studies have shown that there is a strong correlation between the presence and size of an appendicolith with complicated appendicitis [73, 74].

An abdominal aortic aneurysm (AAA) is a focal dilatation of the abdominal aorta measuring greater than 3 cm. Risk factors include smoking as well as connective tissue disorders including Marfan and Ehlers-Danlos syndromes [75]. On plain film, long-standing aneurysms tend to calcify, and can be seen bulging lateral to the lateral borders of the spine (Fig. 30) [72].

Many abdominal vessels can calcify (Fig. 31). Typically, calcification results from atherosclerosis—deposition of fatty materials within the arterial wall that

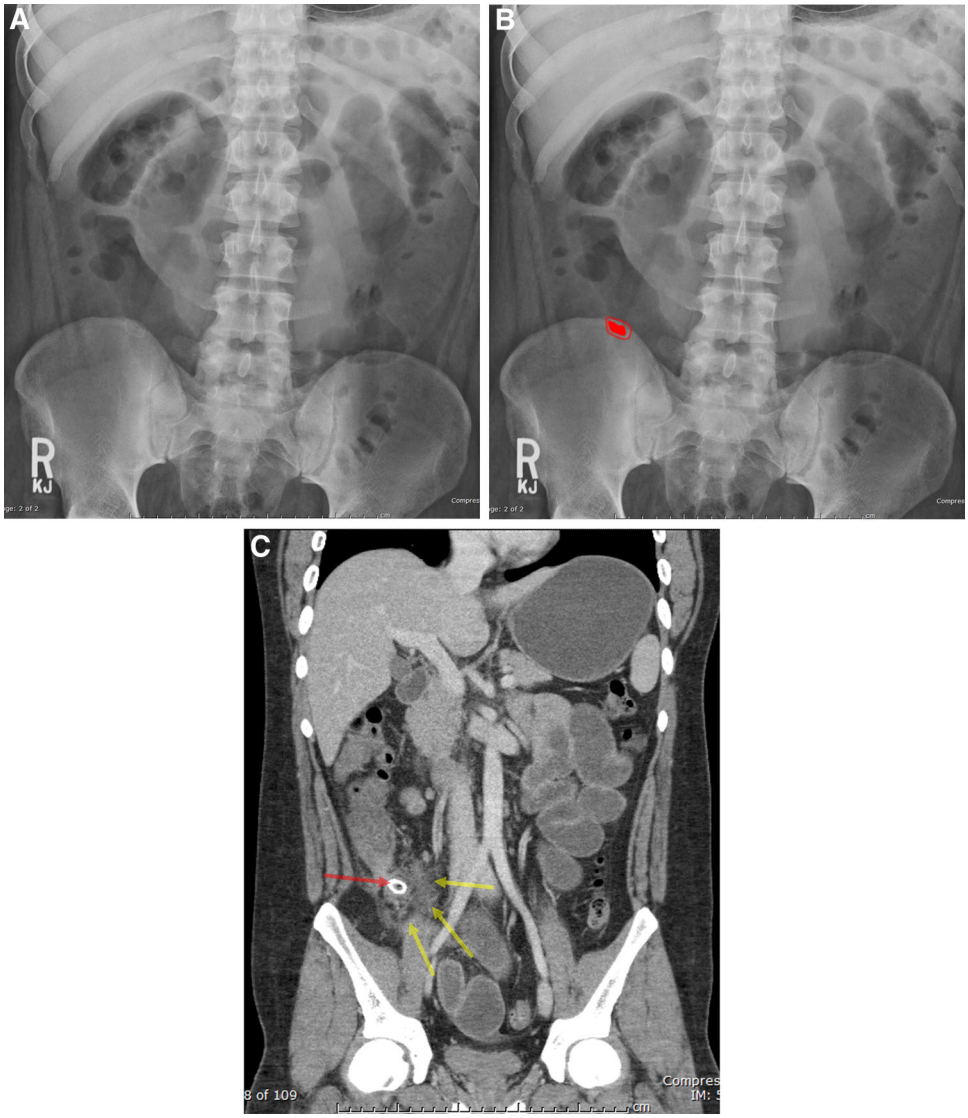

Fig. 29. **A** Abdominal radiograph demonstrating an appendicolith. **B** Lamellate appendicolith in the *right lower* quadrant (*red*). **C** Coronal CT of abdomen revealing an appendicolith (*red arrow*) within an inflamed appendix with surrounding periappendiceal inflammatory changes (*yellow*).

calcifies as the lesion ages. Splenic artery calcifications are more multifactorial, and less often atherosclerotic [76]. On plain film, splenic artery calcifications are tortuous, serpentine, and in the left upper quadrant. Vascular calcifications of the internal iliac arteries in the pelvis also appear tubular; such a small-vessel predominant pattern suggests the presence of diabetes or renal disease [72].

Foreign bodies and iatrogenic pathology

Various implanted devices and nonmedical foreign bodies can be present on abdominal plain films (Fig. 32). Location and orientation can help specify the implant type. For example, a common bile duct (CBD) stent can be differentiated from a transjugular intrahepatic por-

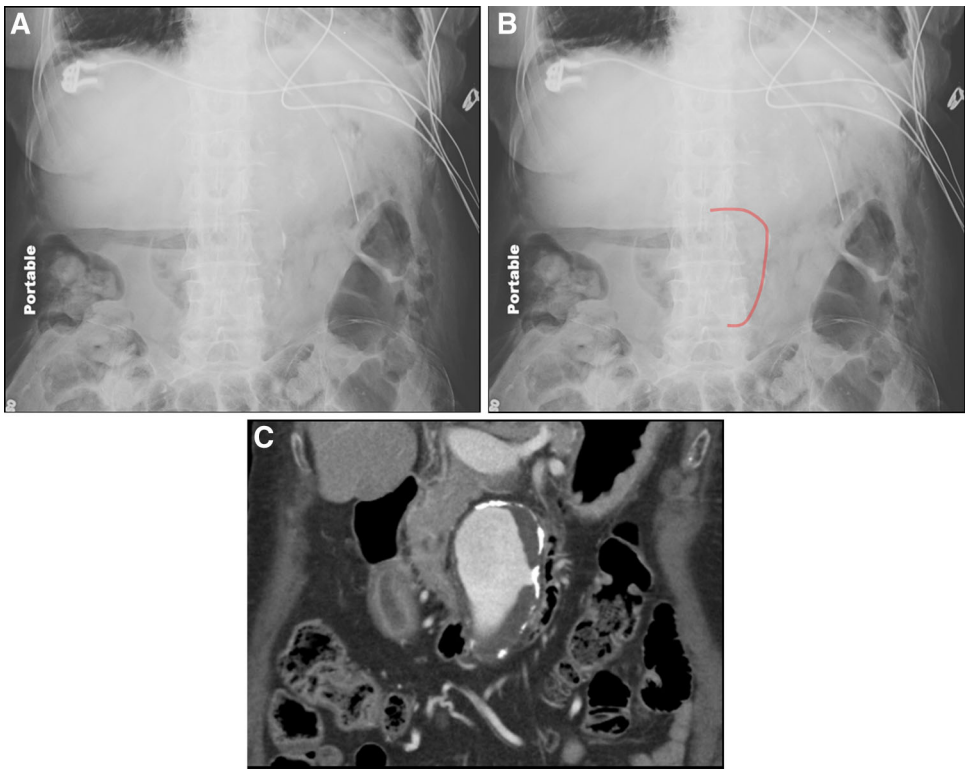

Fig. 30. **A** Abdominal radiograph demonstrating calcified abdominal aortic aneurysm. **B** Calcified wall of an abdominal aortic aneurysm (*red*). **C** Coronal CT on soft tissue windows correlate of the abdominal aortic aneurysm demonstrating calcified plaque and mural thrombus.

tocaval shunt (TIPS) due to the more inferior position and medial curvature of the CBD stent as it courses toward the Sphincter of Oddi to meet the 2nd portion of the duodenum. A typical TIPS is more superior in position and curves laterally as it anastomoses a portal vein with a hepatic vein [77].

Aortic stent grafts are commonly visualized devices in older patients with abdominal aortic aneurysms or prior dissections (Fig. 32). Abdominal plain film can detect certain changes in an endograft more easily than CT. Postoperative complications include stent expansion, migration, kinking, dislocation, and fracture. Care should be taken to assess for positioning variation from prior comparison films, which can affect accurate interpretation [78].

Ureteral stents are inserted by urologists to keep the ureters patent either for the passage of stones or relief of urinary obstruction from mass lesions. Commonly used stents have proximal and distal pigtail loops to prevent migration, with the proximal pigtail placed in the renal pelvis and the distal pigtail in the bladder. Stents may be left in place briefly for a few days up to the duration of the patient's life if needed for malignant disease. Regardless of duration, they should be replaced at 3–6 month intervals. Highly lithogenic urine in concert with prolonged indwelling stent times increases the risk for encrustation, which would appear as irregular calcified densities along the stent path. Encrustation can complicate stent removal and increase the risk of stent fracture. Some degree of encrustation is seen in up to 76.3% of stents placed longer than 12 weeks [79]. As a marker of the ureter course, they can be displaced medially by retroperitoneal fibrosis or laterally by bulky lymphadenopathy (Fig. 33).

Nasogastric (NG) tubes, Dobhoff feeding tubes and ventriculoperitoneal (VP) shunts should be described to indicate their approach and approximate endpoint (Fig. 34). Dobhoff feeding tubes have a radiopaque weighted tip used to aid its positioning beyond the pylorus. Ideal placement is in the 2nd or 3rd portions of the duodenum. Placement within the stomach increases the risk for aspiration [80].

NG tubes have a tip and distal side-port which both should be several centimeters below the gastroesophageal

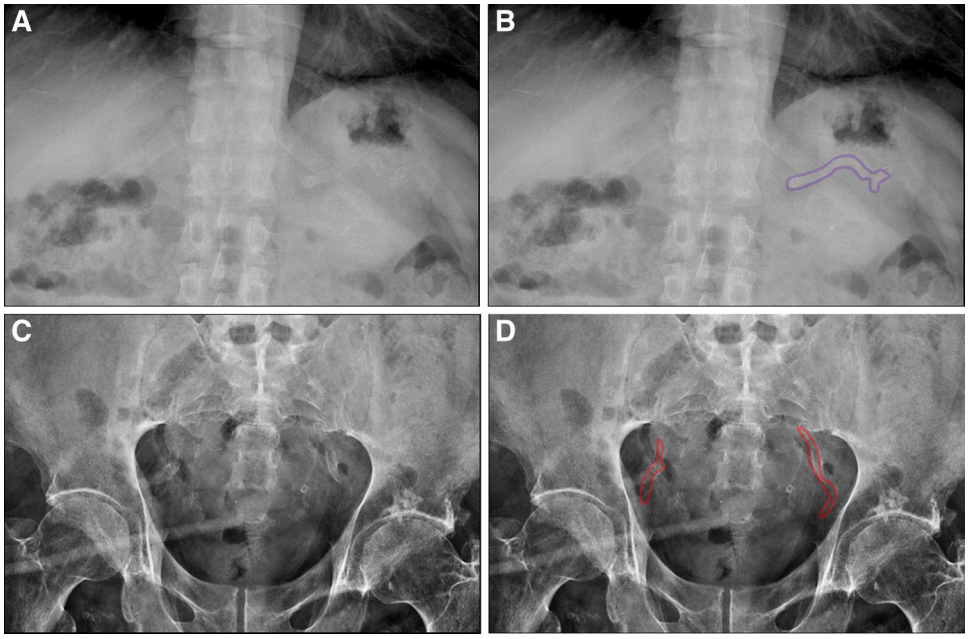

Fig. 31. **A** Abdominal radiograph demonstrating splenic artery calcification. **B** Tubular splenic artery calcification in the *left upper* quadrant (*purple*). **C** Bilateral iliac artery calcification. **D** Tubular iliac artery calcification in the pelvis (*red*).

junction to minimize the chance of reflux and aspiration if the tube is used for feeding. If the NG tube is being used for aspiration, the tip and side-port should be in the most dependent portions of the stomach. Vomiting can occur if the tip curves and presses against the gastric cardia. A decubital sore can occur if the tube is pressed against the fundus [81].

Gastrostomy tubes can be of varying length and appearance depending on whether they were placed surgically, endoscopically, or under fluoroscopic guidance by a radiologist. They should be overlying the expected location of the stomach and an inflated balloon tip may be seen, preventing the tube from pulling out. Intraluminal position cannot be confirmed without the administration of contrast through the tube.

For VP shunts, the presence of any kinks or breaks should be noted. Rectal and Foley catheters both overly the pelvis and may be best identified with the aid of clinical information given their overlapping appearance [77].

Intrauterine devices are commonly seen on plain film overlying the lower pelvis, with varying orientations depending on the direction the uterus is flexed. Breaks in the device can occasionally be seen and a substantial migration of a device from the expected location of the uterus should raise suspicion for malpositioning or erosion into the peritoneal cavity (Fig. 35). Extrauterine migration can be due to uterine perforation or expulsion into the endocervical canal or vagina [82]. Uterine perforation can be life threatening and may require emergent treatment.

There are numerous possible appearances of ingested and inserted nonmedical foreign bodies (Fig. 36). Many foreign bodies, including metal, glass, and stone are opaque and can be detected on plain film. However, CT is more sensitive to detect foreign bodies surrounded by air (as in the bowel), and ultrasound can be useful to detect radiolucent or superficial foreign bodies [83].

Many variants of acupuncture are performed in Eastern medicine. Needles can vary in appearance and may be straight, curvilinear, or semicircular. Sometimes needles are intentionally broken off in the subcutaneous tissues under the assumption that the retained needles will continue to provide stimuli [84].

Contrast nephropathy is defined as an absolute increase in serum creatinine of 0.5 mg/dL, or a 25% increase from the patient's baseline value, within 2–3 days following IV contrast administration [85]. On plain film, a persistent nephrogram is common (Fig. 37) [86]. Both kidneys appear higher in density due to the retention and delayed clearance of radiopaque contrast within the renal tissues. The delay in clearance suggests poor renal function.

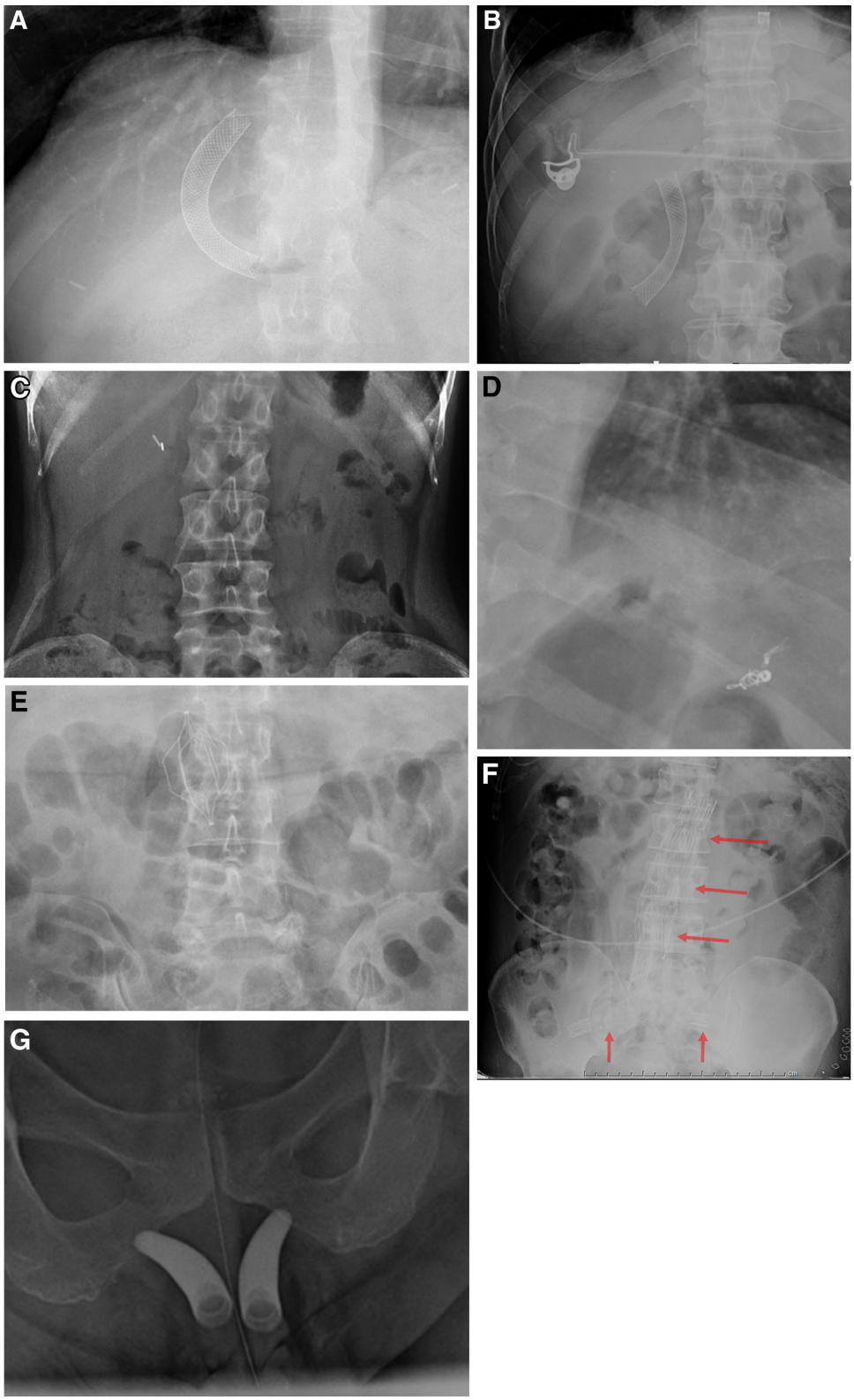

Fig. 32. **A** Abdominal radiograph demonstrating transjugular intrahepatic portocaval shunt (TIPS). **B** Common bile duct stent. **C** Pancreatic duct stent. **D** Embolization coils. **E** IVC filter. **F** Intact aortic stent graft extending into the bilateral iliac arteries (*red arrows*). **G** Penile implant.

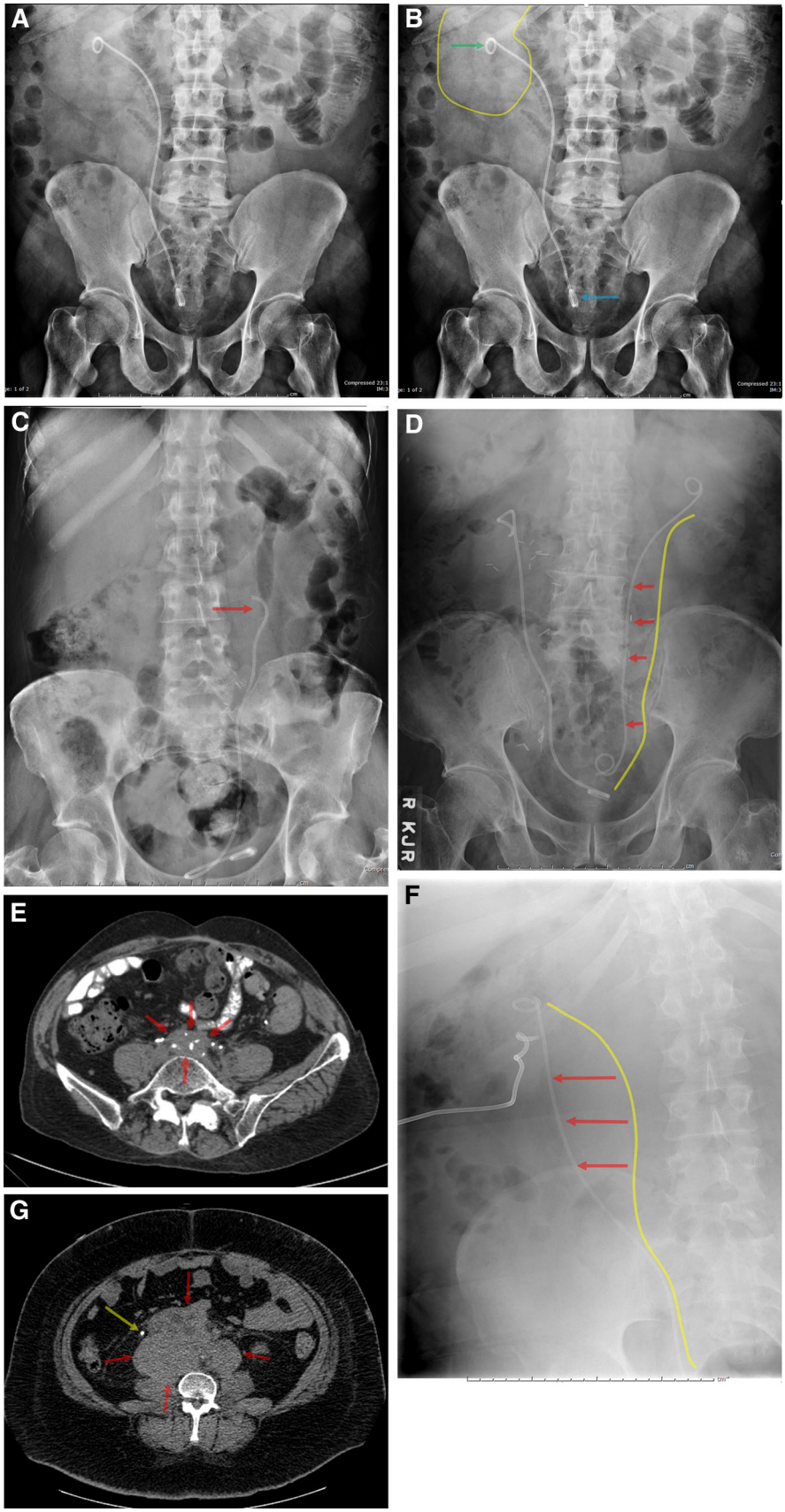

Fig. 33. **A** Normal placement of right-sided ureteral stent. **B** Right renal silhouette (*yellow*), proximal pigtail overlying renal pelvis (*green arrow*), distal pigtail overlying bladder (*blue arrow*). **C** Distal migration of a left ureteral stent with uncoiling of the proximal pigtail (*red arrow*) as it slipped from the renal pelvis to the proximal ureter. **D** Bilateral ureteral stents with medial displacement of the left ureter (*red arrows*) due to retroperitoneal fibrosis. Expected course of the left ureter (*yellow*). **E** Axial CT showing retroperitoneal soft tissue (*red arrows*) surrounding the aorta consistent with fibrosis. **F** Lateral displacement (*red arrows*) of a right ureteral stent due to extensive retroperitoneal lymphadenopathy. Expected course of the left ureter (*yellow*). **G** Axial CT showing bulky retroperitoneal lymphadenopathy (*red arrows*) displacing the stent (*yellow arrow*) laterally.

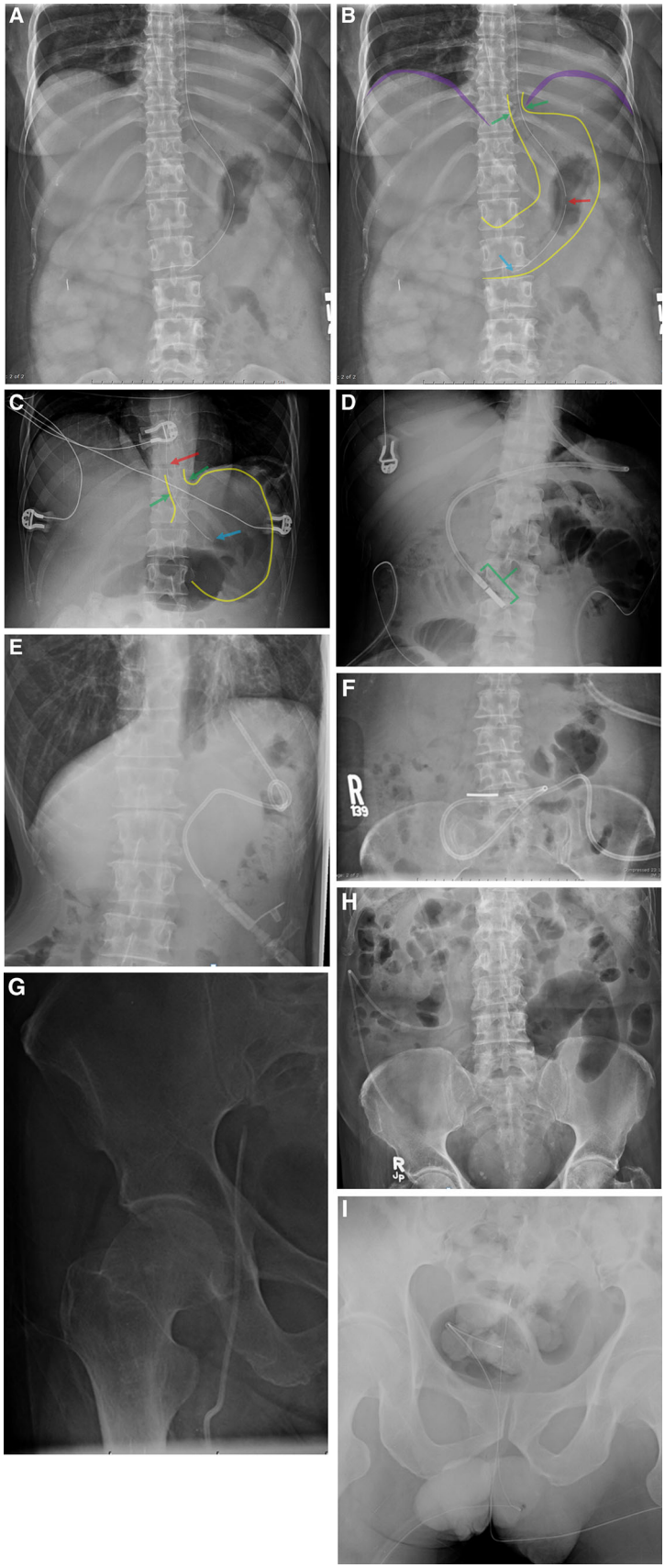

Fig. 34. **A** Proper positioning of a NG tube. **B** Diaphragm (*purple*), gastroesophageal junction (*green arrows*), stomach (*yellow*), side-port (*red arrow*), NG tube tip (*blue arrow*). **C** Improper NG tube with side-port (*red arrow*) and tip (*blue arrow*) above the gastroesophageal junction (*orange*), requiring advancement. **D** Dobhoff feeding tube with weighted tip in the 3rd portion of the duodenum (*green bracket*). **E** Gastrostomy tube. **F** Jejunal feeding tube. **G** Femoral catheter. **H** Ventriculoperitoneal (VP) shunt. **I** Rectal probe and Foley catheter.

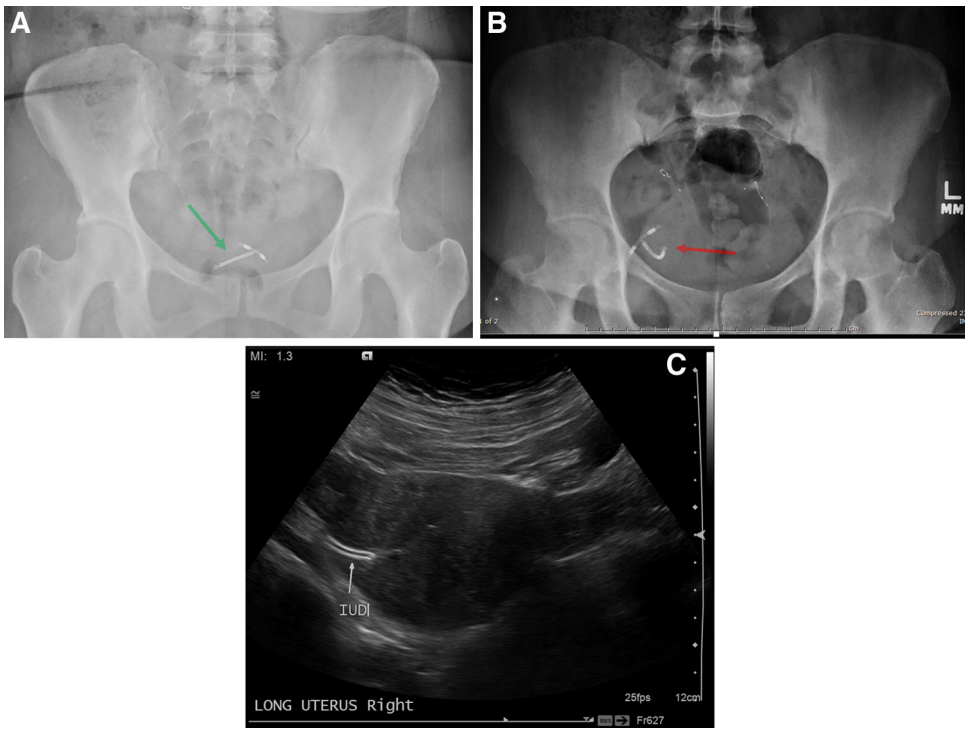

Fig. 35. **A** Abdominal radiograph demonstrating the expected location of an IUD (*green arrow*). **B** Abdominal radiograph showing an IUD overlying the right pelvis (*red arrow*), away from the expected location of the uterus. **C** Sagittal ultrasound image of the uterus showing a portion of the IUD (*white arrow*) eroding through the uterine wall.

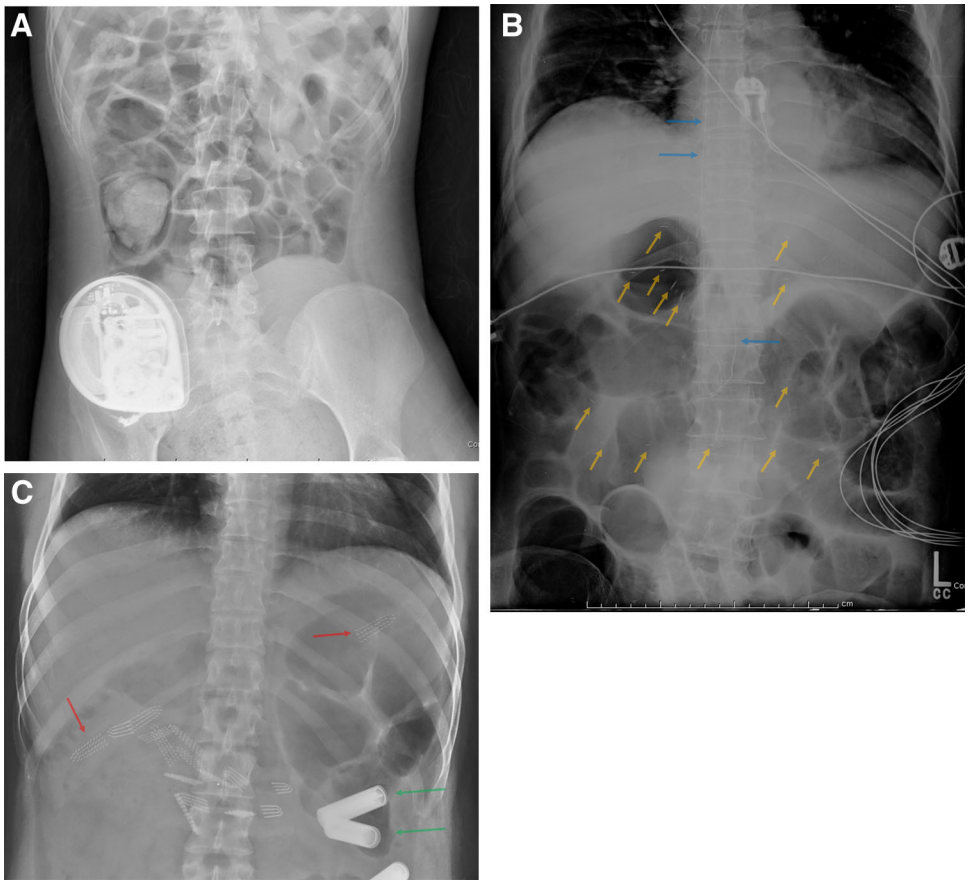

Fig. 36. **A** Abdominal radiograph demonstrating a nerve stimulator. **B** Epidural catheter (*blue arrows*) and acupuncture needles (*orange arrows*). **C** AA batteries (*green arrows*) and toothbrush heads (*red arrows*).

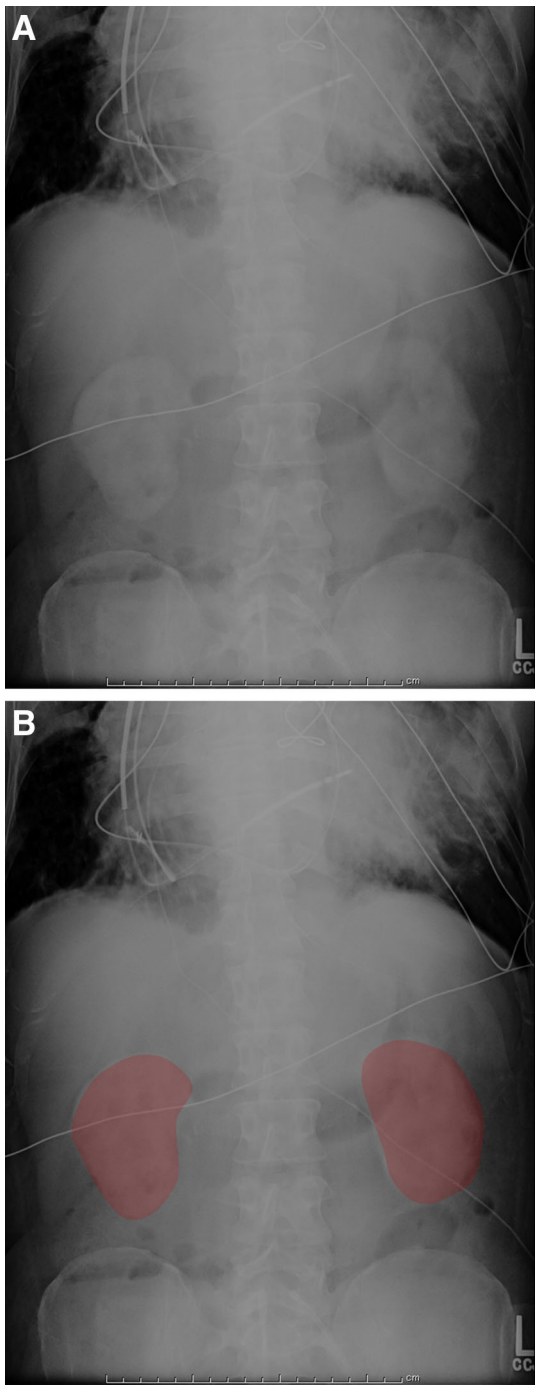

Fig. 37. **A** Abdominal radiograph demonstrating contrast nephropathy. **B** Outlined dense kidneys (*red*).

Conclusions

Abdominal plain films are often the initial examination performed in ED patients with abdominal pain. Proper interpretation can guide early diagnosis as well as prompt advanced imaging. By recognizing the variations of gas patterns—both intraluminal and extraluminal—the radiologist can identify and localize abdominal pathology. In addition, calcifications, medical devices, and foreign bodies can often be confidently diagnosed on abdominal radiography. Although the use of plain film has been superseded by CT for many acute abdominal pathologies in the ED, greater familiarity and confidence with subtle plain film findings may add value to the examination and help guide ED physician on decision making in intangible ways.

Compliance with Ethical Standards

Conflicts of Interest The authors declare that they have no conflict of interest.

Ethical approval All procedures performed in studies involving human participants were in accordance with the ethical standards of the institutional and/or national research committee and with the 1964 Helsinki declaration and its later amendments or comparable ethical standards. For this type of study formal consent is not required. This article does not contain any studies with animals performed by any of the authors.

References

1. Ditkofsky NG, Singh A, Avery L, Novelline RA (2014) The role of emergency MRI in the setting of acute abdominal pain. Emerg Radiol 21(6):615–624. doi:10.1007/s10140-014-1232-2
2. Stoker J, van Randen A, Lameris W, Boermeester MA (2009) Imaging patients with acute abdominal pain. Radiology 253(1):31–46. doi:10.1148/radiol.2531090302
3. Rao PM, Rhea JT, Rao JA, Conn AK (1999) Plain abdominal radiography in clinically suspected appendicitis: diagnostic yield, resource use, and comparison with CT. Am J Emerg Med 17(4):325–328
4. Kellow ZS, MacInnes M, Kurzencwyg D, et al. (2008) The role of abdominal radiography in the evaluation of the nontrauma emergency patient. Radiology 248(3):887–893. doi:10.1148/radiol.2483071772
5. van Randen A, Lameris W, Luitse JS, et al. (2011) The role of plain radiographs in patients with acute abdominal pain at the ED. Am J Emerg Med 29(6):582–589 e582.. doi:10.1016/j.ajem.2009.12.020
6. Eisenberg RL (2008) The role of abdominal radiography in the evaluation of the nontrauma emergency patient: new thoughts on an old problem. Radiology 248(3):715–716. doi:10.1148/radiol.2483080863
7. Pinto A, Lanza C, Pinto F, et al. (2015) Role of plain radiography in the assessment of ingested foreign bodies in the pediatric patients. Semin Ultrasound CT MR 36(1):21–27. doi:10.1053/j.sult.2014.10.008
8. Baker N, Woolridge D (2013) Emerging concepts in pediatric emergency radiology. Pediatr Clin North Am 60(5):1139–1151. doi:10.1016/j.pcl.2013.06.004
9. James B, Kelly B (2013) The abdominal radiograph. Ulster Med J 82(3):179–187
10. Brenner DJ, Hall EJ (2007) Computed tomography–an increasing source of radiation exposure. N Engl J Med 357(22):2277–2284. doi:10.1056/NEJMra072149
11. Nair N, Takieddine Z, Tariq H (2015) Colonic interposition between the liver and right diaphragm: the 'Chilaiditi sign'. Can J Gastroenterol Hepatol
12. Bohm B, Milsom JW, Fazio VW (1995) Postoperative intestinal motility following conventional and laparoscopic intestinal surgery. Arch Surg 130(4):415–419
13. Kammen BF, Levine MS, Rubesin SE, Laufer I (2000) Adynamic ileus after caesarean section mimicking intestinal obstruction: findings on abdominal radiographs. Br J Radiol 73(873):951–955. doi:10.1259/bjr.73.873.11064647
14. Kim SH, Park KN, Kim SJ, et al. (2011) Accuracy of plain abdominal radiography in the differentiation between small bowel obstruction and small bowel ileus in acute abdomen presenting to emergency department. Hong Kong J Emerg Med 18(2):68–79
15. Spurk JH (1997) *Fluid mechanics*. New York: Springer

16. Davis S, Parbhoo SP, Gibson MJ (1980) The plain abdominal radiograph in acute pancreatitis. Clin Radiol 31(1):87–93
17. Silva AC, Pimenta M, Guimaraes LS (2009) Small bowel obstruction: what to look for. Radiographics 29(2):423–439. doi:10.1148/rg.292085514
18. Maglinte DD, Balthazar EJ, Kelvin FM, Megibow AJ (1997) The role of radiology in the diagnosis of small-bowel obstruction. AJR Am J Roentgenol 168(5):1171–1180. doi:10.2214/ajr.168.5.9129407
19. Miyazaki O (1995) Efficacy of abdominal plain film and CT in bowel obstruction. Nihon Igaku Hoshasen Gakkai Zasshi 55(4):233–239
20. Frager D, Medwid SW, Baer JW, Mollinelli B, Friedman M (1994) CT of small-bowel obstruction: value in establishing the diagnosis and determining the degree and cause. AJR Am J Roentgenol 162(1):37–41. doi:10.2214/ajr.162.1.8273686
21. Maglinte DD, Reyes BL, Harmon BH, et al. (1996) Reliability and role of plain film radiography and CT in the diagnosis of small-bowel obstruction. AJR Am J Roentgenol 167(6):1451–1455. doi:10.2214/ajr.167.6.8956576
22. Harlow CL, Stears RL, Zeligman BE, Archer PG (1993) Diagnosis of bowel obstruction on plain abdominal radiographs: significance of air-fluid levels at different heights in the same loop of bowel. AJR Am J Roentgenol 161(2):291–295. doi:10.2214/ajr.161.2.8333364
23. Thompson WM (2008) Gasless abdomen in the adult: what does it mean? AJR Am J Roentgenol 191(4):1093–1099. doi:10.2214/AJR.07.3837
24. Hayakawa K, Tanikake M, Yoshida S, et al. (2013) Radiological diagnosis of large-bowel obstruction: neoplastic etiology. Emerg Radiol 20(1):69–76. doi:10.1007/s10140-012-1088-2
25. Slam KD, Calkins S, Cason FD (2007) LaPlace's law revisited: cecal perforation as an unusual presentation of pancreatic carcinoma. World J Surg Oncol 5:14. doi:10.1186/1477-7819-5-14
26. Gingold D, Murrell Z (2012) Management of colonic volvulus. Clin Colon Rectal Surg 25(4):236–244. doi:10.1055/s-0032-1329535
27. Jaffe T, Thompson WM (2015) Large-bowel obstruction in the adult: classic radiographic and CT findings, etiology, and mimics. Radiology 275(3):651–663. doi:10.1148/radiol.2015140916
28. Tiah L, Goh SH (2006) Sigmoid volvulus: diagnostic twists and turns. Eur J Emerg Med 13(2):84–87. doi:10.1097/01.mej.0000190278.30850.8a
29. Feldman D (2000) The coffee bean sign. Radiology 216(1):178–179. doi:10.1148/radiology.216.1.r00jl17178
30. Burrell HC, Baker DM, Wardrop P, Evans AJ (1994) Significant plain film findings in sigmoid volvulus. Clin Radiol 49(5):317–319
31. Javors BR, Baker SR, Miller JA (1999) The northern exposure sign: a newly described finding in sigmoid volvulus. AJR Am J Roentgenol 173(3):571–574. doi:10.2214/ajr.173.3.10470881
32. Delabrousse E, Sarlieve P, Sailley N, Aubry S, Kastler BA (2007) Cecal volvulus: CT findings and correlation with pathophysiology. Emerg Radiol 14(6):411–415. doi:10.1007/s10140-007-0647-4
33. Lopez Perez E, Martinez Perez MJ, Ripolles Gonzalez T, Vila Miralles R, Flors Blasco L (2010) Cecal volvulus: imaging features. Radiologia 52(4):333–341. doi:10.1016/j.rx.2010.03.014
34. Coulie B, Camilleri M (1999) Intestinal pseudo-obstruction. Annu Rev Med 50:37–55. doi:10.1146/annurev.med.50.1.37
35. De Giorgio R, Knowles CH (2009) Acute colonic pseudo-obstruction. Br J Surg 96(3):229–239. doi:10.1002/bjs.6480
36. Lang EV, Carson L, Gossler A (1998) Gas lock obstruction of the colon: Ogilvie's syndrome revisited. AJR Am J Roentgenol 171(4):1014–1016. doi:10.2214/ajr.171.4.9762987
37. Low VH (1995) Colonic pseudo-obstruction: value of prone lateral view of the rectum. Abdom Imaging 20(6):531–533
38. Mounsey A, Raleigh M, Wilson A (2015) Management of constipation in older adults. Am Fam Physician 92(6):500–504
39. Hussain ZH, Whitehead DA, Lacy BE (2014) Fecal impaction. Curr Gastroenterol Rep 16(9):404. doi:10.1007/s11894-014-0404-2
40. Saksonov M, Bachar GN, Morgenstern S, et al. (2014) Stercoral colitis: a lethal disease-computed tomographic findings and clinical characteristic. J Comput Assist Tomogr 38(5):721–726. doi:10.1097/RCT.0000000000000117
41. Cunha TB, Tahan S, Soares MF, Lederman HM, Morais MB (2012) Abdominal radiograph in the assessment of fecal impaction in children with functional constipation: comparing three scoring systems. J Pediatr (Rio J) 88(4):317–322. doi:10.2223/JPED.2199
42. Cowlam S, Vinayagam R, Khan U, et al. (2008) Blinded comparison of faecal loading on plain radiography versus radio-opaque marker transit studies in the assessment of constipation. Clin Radiol 63(12):1326–1331. doi:10.1016/j.crad.2008.06.011
43. Bartram CI (1976) Plain abdominal X-ray in acute colitis. Proc R Soc Med 69(8):617–618
44. Gore RM, Levine MS, Laufer I (1994) *Textbook of gastrointestinal radiology*. Philadelphia: W.B. Saunders Co.
45. Prantera C, Lorenzetti R, Cerro P, et al. (1991) The plain abdominal film accurately estimates extent of active ulcerative colitis. J Clin Gastroenterol 13(2):231–234
46. O'Regan K, O'Connor OJ, O'Neill SB, et al. (2012) Plain abdominal radiographs in patients with Crohn's disease: radiological findings and diagnostic value. Clin Radiol 67(8):774–781. doi:10.1016/j.crad.2012.01.005
47. Kawamoto S, Horton KM, Fishman EK (1999) Pseudomembranous colitis: spectrum of imaging findings with clinical and pathologic correlation. Radiographics 19(4):887–897. doi:10.1148/radiographics.19.4.g99jl07887
48. Autenrieth DM, Baumgart DC (2012) Toxic megacolon. Inflamm Bowel Dis 18(3):584–591. doi:10.1002/ibd.21847
49. Boyer TD, Wright TL, Manns MP, Zakim D (2006) *Zakim and Boyer's hepatology: a textbook of liver disease*, 5th edn. Philadelphia, PA: Saunders/Elsevier
50. Kaude JV, DeLand F (1975) Hepatomegaly. Med Clin North Am 59(1):145–167
51. O'Reilly RA (1996) Splenomegaly at a United States County Hospital: diagnostic evaluation of 170 patients. Am J Med Sci 312(4):160–165
52. Quiroga O, Matozzi F, Beranger M, et al. (1982) Normal CT anatomy of the spine. Anatomo-radiological correlations. Neuroradiology 24(1):1–6
53. Bundrick TJ, Cho SR, Brewer WH, Beachley MC (1984) Ascites: comparison of plain film radiographs with ultrasonograms. Radiology 152(2):503–506. doi:10.1148/radiology.152.2.6739823
54. Lee CH (2010) Images in clinical medicine. Radiologic signs of pneumoperitoneum. N Engl J Med 362(25):2410. doi:10.1056/NEJMicm0904627
55. Chapman BC, McIntosh KE, Jones EL, et al. (2015) Postoperative pneumoperitoneum: is it normal or pathologic? J Surg Res 197(1):107–111. doi:10.1016/j.jss.2015.03.083
56. Feczko PJ, Mezwa DG, Farah MC, White BD (1992) Clinical significance of pneumatosis of the bowel wall. Radiographics 12(6):1069–1078. doi:10.1148/radiographics.12.6.1439012
57. Soyer P, Martin-Grivaud S, Boudiaf M, et al. (2008) Linear or bubbly: a pictorial review of CT features of intestinal pneumatosis in adults. J Radiol 89(12):1907–1920
58. Sebastia C, Quiroga S, Espin E, et al. (2000) Portomesenteric vein gas: pathologic mechanisms, CT findings, and prognosis. Radiographics 20 (5):1213–1224; discussion 1224–1216. doi:10.1148/radiographics.20.5.g00se011213
59. Rajkovic Z, Papes D, Altarac S, Arslani N (2013) Differential diagnosis and clinical relevance of pneumobilia or portal vein gas on abdominal X-ray. Acta Clin Croat 52(3):369–373
60. Brandon JC, Glick SN, Teplick SK, Silverstein GS (1988) Emphysematous cholecystitis: pitfalls in its plain film diagnosis. Gastrointest Radiol 13(1):33–36. doi:10.1007/BF01889020
61. Wan YL, Lee TY, Bullard MJ, Tsai CC (1996) Acute gas-producing bacterial renal infection: correlation between imaging findings and clinical outcome. Radiology 198(2):433–438. doi:10.1148/radiology.198.2.8596845
62. Bliznak J, Ramsey J (1972) Emphysematous pyelonephritis. Clin Radiol 23(1):61–64
63. Narlawar RS, Raut AA, Nagar A, et al. (2004) Imaging features and guided drainage in emphysematous pyelonephritis: a study of 11 cases. Clin Radiol 59(2):192–197
64. Grupper M, Kravtsov A, Potasman I (2007) Emphysematous cystitis: illustrative case report and review of the literature. Medicine (Baltimore) 86(1):47–53. doi:10.1097/MD.0b013e3180307c3a
65. Gordon R (1980) The deep sulcus sign. Radiology 136(1):25–27. doi:10.1148/radiology.136.1.7384513

66. Coursey CA, Casalino DD, Remer EM, et al. (2012) ACR Appropriateness Criteria(R) acute onset flank pain–suspicion of stone disease. Ultrasound Q 28(3):227–233. doi:10.1097/RUQ.0b013e3182625974
67. Traubici J, Neitlich JD, Smith RC (1999) Distinguishing pelvic phleboliths from distal ureteral stones on routine unenhanced helical CT: is there a radiolucent center? AJR Am J Roentgenol 172(1):13–17. doi:10.2214/ajr.172.1.9888730
68. Jindal G, Ramchandani P (2007) Acute flank pain secondary to urolithiasis: radiologic evaluation and alternate diagnoses. Radiol Clin North Am 45(3):395–410., vii. doi:10.1016/j.rcl.2007.04.001
69. Baron RL (1991) Gallstone characterization: the role of imaging. Semin Roentgenol 26(3):216–225
70. Etemad B, Whitcomb DC (2001) Chronic pancreatitis: diagnosis, classification, and new genetic developments. Gastroenterology 120(3):682–707
71. Present AJ, Geyman MJ (1947) Diffuse calcification of the pancreas. Radiology 48(1):29–32. doi:10.1148/48.1.29
72. Baker SR (1990) *The abdominal plain film*. Norwalk: Appleton & Lange
73. Guy PJ, Pailthorpe CA (1983) The radio-opaque appendicolith–its significance in clinical practice. J R Army Med Corps 129(3):163–166
74. Ishiyama M, Yanase F, Taketa T, et al. (2013) Significance of size and location of appendicoliths as exacerbating factor of acute appendicitis. Emerg Radiol 20(2):125–130. doi:10.1007/s10140-012-1093-5
75. Ernst CB (1993) Abdominal aortic aneurysm. N Engl J Med 328(16):1167–1172. doi:10.1056/NEJM199304223281607
76. Golder WA (2008) Tortuosity and calcification of the splenic artery. More than an additional finding. Radiologe 48(11):1066–1067. doi:10.1007/s00117-008-1631-z
77. Hunter TB, Taljanovic MS (2005) Medical devices of the abdomen and pelvis. Radiographics 25(2):503–523. doi:10.1148/rg.252045157
78. Fearn S, Lawrence-Brown MM, Semmens JB, Hartley D (2003) Follow-up after endovascular aortic aneurysm repair: the plain radiograph has an essential role in surveillance. J Endovasc Ther 10(5):894–901. doi:10.1583/1545-1550(2003)010<0894:FAEAAR>2.0.CO;2
79. Dyer RB, Chen MY, Zagoria RJ, et al. (2002) Complications of ureteral stent placement. Radiographics 22(5):1005–1022. doi:10.1148/radiographics.22.5.g02se081005
80. Gharib AM, Stern EJ, Sherbin VL, Rohrmann CA (1996) Nasogastric and feeding tubes. The importance of proper placement. Postgrad Med 99(5):165–168
81. Niv Y, Abu-Avid S (1988) On the positioning of a nasogastric tube. Am J Med 84(3 Pt 1):563–564
82. Carmody K, Schwartz B, Chang A (2011) Extrauterine migration of a mirena(R) intrauterine device: a case report. J Emerg Med 41(2):161–165. doi:10.1016/j.jemermed.2010.04.024
83. Aras MH, Miloglu O, Barutcugil C, et al. (2010) Comparison of the sensitivity for detecting foreign bodies among conventional plain radiography, computed tomography and ultrasonography. Dentomaxillofac Radiol 39(2):72–78. doi:10.1259/dmfr/68589458
84. Gerard PS, Wilck E, Schiano T (1993) Imaging implications in the evaluation of permanent needle acupuncture. Clin Imaging 17(1):36–40
85. Pucelikova T, Dangas G, Mehran R (2008) Contrast-induced nephropathy. Catheter Cardiovasc Interv 71(1):62–72. doi:10.1002/ccd.21207
86. Older RA, Korobkin M, Cleeve DM, Schaaf R, Thompson W (1980) Contrast-induced acute renal failure: persistent nephrogram as clue to early detection. AJR Am J Roentgenol 134(2):339–342. doi:10.2214/ajr.134.2.339